On the relaxation of a two-level system driven by a strong electromagnetic field

Eitan Geva and Ronnie Kosloff
Department of Physical Chemistry and the Fritz Haber Research Center, the Hebrew University, Jerusalem 91904, Israel

J. L. Skinner
Theoretical Chemistry Institute and Department of Chemistry, University of Wisconsin, Madison, Wisconsin 53706

(Received 2 December 1994; accepted 24 February 1995)

A detailed and unified account of the theory of the generalized Bloch equations is presented. The equations apply to a two-level system weakly coupled to a heat bath and subject to a monochromatic rotating field of arbitrary intensity. The relaxation tensor obtained is explicitly field-dependent. The derivation is valid for general coupling to a quantum heat bath. The generalized Bloch equations are shown to be thermodynamically consistent, as opposed to the standard Bloch equations. Different limits of the generalized Bloch equations are examined and related to previous studies. The potential use of the generalized Bloch equations as a probe of the bath spectral density is demonstrated for the case of a two-level system embedded in a Debye solid. © *1995 American Institute of Physics.*

I. INTRODUCTION

In 1946 Bloch proposed the differential equations

$$\frac{d\mathbf{M}}{dt}=\gamma\mathbf{M}\times\mathscr{H}-\frac{M_x}{T_2}\,\hat{\mathbf{x}}-\frac{M_y}{T_2}\,\hat{\mathbf{y}}-\frac{(M_z-M_z^{eq})}{T_1}\,\hat{\mathbf{z}} \qquad (1.1)$$

to describe the motion of the components of the macroscopic nuclear polarization, **M**, subject to an external, possibly time-dependent, magnetic field, $\mathscr{H}$.[1] Bloch and Wangsness,[2] Redfield,[3] and others[4–6] later derived these equations in the limit of weak coupling to the bath *and* the external field. In these derivations the nuclear spins and the heat bath were considered as quantum mechanical entities, semiclassically driven by the time-dependent field. The interaction with the driving field was treated in the limit of linear response theory,[7] where it only affected the Hamiltonian contribution to the dynamics, and the dissipative, non-Hamiltonian contribution remained field-independent.

Equations of the form of Eq. (1.1) were later successfully applied to other branches of spectroscopy,[8,9] far exceeding the original context for which they were first suggested. In the most common usage, two of the energy levels of a system are isolated, and a fictitious spin-1/2 is associated with them.[10] This two-level system (TLS) paradigm has played a fundamental role in the development of spectroscopy. The general features of the derivation and interpretation of the Bloch equations remain similar to those in magnetic resonance, although the application to other resonance phenomena has forced researchers to abandon the high-temperature limit (often used in magnetic resonance theory), and to consider new relaxation mechanisms.[11–17]

As early as 1955 Redfield demonstrated that the Bloch equations fail to explain the experimental behavior of spin systems close to saturation, i.e. when subject to high fields. Redfield proposed a resolution of this problem in terms of a spin temperature in the rotating frame.[5,18] Bloch,[19] Tomita,[20] Hubbard,[21] and Argyres and Kelley[22] then showed how to derive ''generalized Bloch equations'' that are valid in the case of a rotating transverse field of arbitrary intensity. The generalized Bloch equations (GBE) are stated in terms of the polarization components along the axes of a reference frame rotating with the transverse field. These equations are explicitly derived in the present paper, and the final result is summarized in Eq. (4.34). The main differences between the standard Bloch equations (SBE) and generalized versions (GBE) are: (1) the bath terms become dependent on the frequency and amplitude of the driving field; (2) the relaxation matrix is not diagonal and includes coupling terms between the longitudinal polarization and the component rotating in phase with the transverse field; (3) the equation of motion for the polarization component rotating in phase with the transverse field contains a new inhomogeneous term.

Analogous deviations from the behavior predicted by the SBE were not reported in other branches of spectroscopy until 1983, when DeVoe and Brewer[23] presented experimental evidence for the failure of the SBE to explain the free-induction decay that follows saturation of an electronic transition of $\mathbf{Pr^{3+}}$ impurity in $\mathbf{LaF_3}$ crystal. A similar failure of the SBE was subsequently demonstrated by photon echo experiments on **Yb** vapor.[24] These experiments stimulated researchers to consider generalizations to the standard optical Bloch equations.[25–36] In this paper it will be shown that many of these treatments correspond to a certain limit of the GBE.

From both the magnetic resonance and optical results it is now clear that experimental capabilities enable the exploration of phenomena beyond the limit of linear response theory, naturally leading to the necessity to develop a theory for such circumstances. Thus, the GBE will obviate the questionable use of the SBE to interpret experiments that exploit intense fields.

The proper description of the relaxation dynamics of a system simultaneously interacting with a heat bath and a time-dependent driving field is of fundamental importance for nonequilibrium thermodynamics as well as spectroscopy. Phenomenological thermodynamics, which started as a theory of heat engines,[37] originally sought to understand the bounds imposed on processes in systems interacting with

heat baths while driven by a time-dependent external field.[38] However, starting with the Boltzmann equation,[39] irreversible statistical thermodynamics has been traditionally engaged with systems subject to fixed boundaries. One very important exception is Kubo's linear response theory.[7,40] However, the latter is only valid if the external time-dependent field is considered as a small perturbation. Any general description of the relaxation dynamics beyond the limit of linear response must therefore be consistent with thermodynamics.

The Bloch equations describe a simple example of a system subject to quantum dynamics, while still permitting a straightforward analysis in thermodynamic terms. The requirement for consistency with thermodynamics reduces in this case to the demand that, in steady state, energy will flow from the driving field into the heat bath. The reverse process implying net production of work out of heat, without any further changes in the surroundings, is forbidden by the second law of thermodynamics. It should be noted that this statement of the second law is made in terms of *path* functions, rather than *state* functions. The former can be clearly defined for our model, thereby avoiding the questionable definition of entropy far from equilibrium.

In a previous study a combination of a structure theorem from semigroup theory[41] with the constraint imposed by the requirement for thermodynamical consistency was employed in order to construct an equation of motion for quantum systems simultaneously interacting with heat baths and time-dependent fields.[42–45] The construction of these equations was motivated by a general effort to examine the limitations imposed by quantum dynamics on the performance of heat engines operated in finite time. The treatment in Refs. 42–45 was based upon a fundamental relationship between the thermodynamical work and heat currents and the corresponding quantum observables.[46,47] The structure of these equations was similar to that of the GBE in that they involved field-dependent bath terms, which turned out to be essential for thermodynamic consistency. However, the relaxation equations of Refs. 42–45 are only valid for "slowly" varying fields, whereas the GBE presented here hold for "fast" fields. Hence the two approaches are complementary (cf. Sec. VIII). In the present paper the GBE are re-examined from a thermodynamical point of view.

The organization of this paper is as follows. The basic model of a TLS coupled to a quantum-mechanical heat bath and to a rotating field of arbitrary intensity is presented in Sec. II. The thermodynamic aspects of the model are described in Sec. III. The detailed derivation of the GBE [Eq. (4.34)] is presented in Sec. IV. The conditions under which the GBE reduce to the SBE or to the generalized optical Bloch equations[29,30,32] are considered in Sec. V. The steady-state solution of the GBE is considered in Sec. VI. It is shown that the GBE are consistent with the second law of thermodynamics. The connection to experiment is through the line-shape function, which is also discussed in Sec. VI. An example of the implications of the GBE for the case of a TLS impurity subject to a strong field and embedded in a Debye solid is provided in Sec. VII. Some final remarks involving the relation of this work to other studies are presented in Sec. VIII.

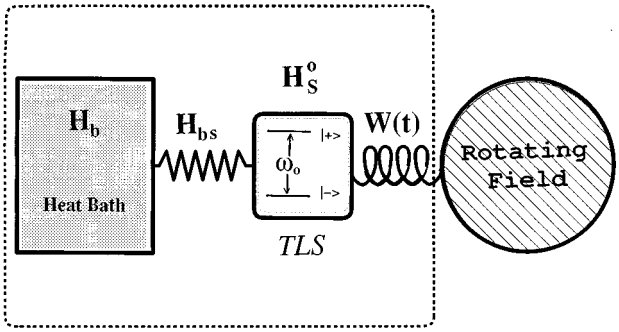

FIG. 1. Schematic view of the model. The TLS, with free Hamiltonian $\mathbf{H_s^0}$ is coupled to a heat bath, with free Hamiltonian $\mathbf{H_b}$, through the interaction Hamiltonian $\mathbf{H_{bs}}$, while subject to a driving term $\mathbf{W}(t)$ by an external monochromatic rotating field. The dashed frame deliminates the extended system consisting of the TLS and bath, which evolves in time according to the Liouville equation.

II. BASIC MODEL

The basic model consists of a TLS, a quantum heat bath, and a monochromatic rotating electromagnetic field. The TLS is simultaneously coupled to the field and the heat bath. Since the field is strong a semiclassical description of the field is sufficient. The model is schematically depicted in Fig. 1.

The state of the extended system, consisting of the TLS and the heat bath, is described by the density operator ρ. The dynamics of ρ is governed by the Liouville von Neumann equation

$$\frac{\partial \rho}{\partial t} = -i[\mathbf{H}(t),\rho] \equiv -i\mathscr{L}(t)\rho, \tag{2.1}$$

where the total Hamiltonian of the extended system is given by

$$\mathbf{H}(t) = \mathbf{H_b} + \mathbf{H_s^0} + \mathbf{W}(t) + \mathbf{H_{bs}}. \tag{2.2}$$

$\mathbf{H_b}$ is the free bath Hamiltonian, which remains unspecified for most of this paper. $\mathbf{H_s^0}$ is the free TLS Hamiltonian

$$\mathbf{H_s^0} = \omega_0 \mathbf{P_z}. \tag{2.3}$$

ω_0 is the *positive* energy gap between the two energy levels (the units are such that $\hbar = 1$). In the language of magnetic resonance ω_0 is the Larmor frequency of the spin's free precession around the z axis. $\mathbf{P_z}$ is a projector defined in Eq. (2.6) below. $\mathbf{W}(t)$ constitutes the semiclassical interaction Hamiltonian of the TLS with a single mode *rotating* field:

$$\mathbf{W}(t) = \epsilon[\mathbf{P}_+ e^{-i\omega t} + \mathbf{P}_- e^{i\omega t}] = 2\epsilon[\mathbf{P_x}\cos(\omega t) + \mathbf{P_y}\sin(\omega t)]. \tag{2.4}$$

ω is the field frequency, and ϵ measures the strength of the TLS-field interaction. ϵ will be referred to as "the amplitude of the field" in the rest of this paper. Also, note that 2ϵ (actually -2ϵ, according to standard usage) is the Rabi frequency. The TLS operators $\mathbf{P}_+$, $\mathbf{P}_-$, $\mathbf{P_x}$ and $\mathbf{P_y}$ are defined in Eq. (2.6) below. For magnetic resonance and certain atomic

transitions Eq. (2.4) can be realized exactly, while for other TLS situations this equation results from making the rotating wave approximation. Note, however, that for very intense fields such that ϵ is comparable to ω_0 the rotating wave approximation is not expected to be valid. The choice of a rotating field yields crucial simplification of the derivation of the GBE. Finally, since the field is circularly polarized, negative frequencies are physically meaningful and distinct from positive ones. Changing the sign of the frequency corresponds to rotating the field in the counter direction.

The TLS-bath interaction Hamiltonian is defined as

$$\mathbf{H_{bs}}=\delta\{\mathbf{\Lambda}\otimes\mathbf{P}_+ + \mathbf{\Lambda}^\dagger\otimes\mathbf{P}_- + \mathbf{\Delta}\otimes\mathbf{P_z}\}. \tag{2.5}$$

δ is a dimensionless coupling parameter that measures the strength of the TLS-bath coupling. $\mathbf{\Lambda}$, $\mathbf{\Lambda}^\dagger$ and $\mathbf{\Delta}$ are bath operators. $\mathbf{H_{bs}}$ must be Hermitian; hence $\mathbf{\Lambda}$, $\mathbf{\Lambda}^\dagger$ are Hermitian conjugates and $\mathbf{\Delta}$ is Hermitian. Without loss of generality, the free bath thermal averages of these operators are chosen to be zero: $\langle\mathbf{\Lambda}\rangle_b=\langle\mathbf{\Lambda}^\dagger\rangle_b=\langle\mathbf{\Delta}\rangle_b=0$, where $\langle\mathbf{\Gamma}\rangle_b\equiv \mathrm{Tr}_b(\boldsymbol{\rho}_\mathbf{b}\mathbf{\Gamma})$ and $\boldsymbol{\rho}_\mathbf{b}\equiv e^{-\beta\mathbf{H_b}}/\mathrm{Tr}_b(e^{-\beta\mathbf{H_b}})$. $\beta=1/T$ is the bath inverse temperature, where T is the bath absolute temperature measured in units of energy ($k_B=1$). Finally, $\mathbf{P_z}$, $\mathbf{P}_+$, $\mathbf{P}_-$, $\mathbf{P_x}$, and $\mathbf{P_y}$ are the TLS operators:

$$\mathbf{P_z}=\tfrac{1}{2}\,(|+\rangle\langle+|-|-\rangle\langle-|), \quad \mathbf{P}_+=|+\rangle\langle-|,$$

$$\mathbf{P}_-=|-\rangle\langle+|,$$

$$\mathbf{P_x}=\frac{1}{2}\,(\mathbf{P}_+ + \mathbf{P}_-), \quad \mathbf{P_y}=\frac{1}{2i}\,(\mathbf{P}_+ - \mathbf{P}_-), \tag{2.6}$$

where $\mathbf{P_z}|\pm\rangle=\pm\tfrac{1}{2}\,|\pm\rangle$. $\mathbf{P}_+$ and $\mathbf{P}_-$ are the creation and annihilation operators of the free TLS and $\mathbf{P_x}$ and $\mathbf{P_y}$ ($\mathbf{P_z}$) correspond to the transverse (longitudinal) polarizations.

III. THERMODYNAMIC CONSIDERATIONS

Thermodynamic considerations are based on a set of assumptions independent of the axioms of quantum mechanics. Therefore they can be used as a validity test of the approximations leading to the quantum master equation.

The derivation of the GBE (cf. Sec. IV) leads to a quantum master equation for any TLS observable, **X,** having the generic form

$$\dot{\mathbf{X}}=i[\mathbf{H_s^0}+\mathbf{W}(t),\mathbf{X}]+\frac{\partial\mathbf{X}}{\partial t}+\mathscr{L}_D^*(\mathbf{X}), \tag{3.1}$$

where $\mathscr{L}_D^*$ is a dissipation super-operator representing the dissipative dynamics induced by the heat bath. The specific form of $\mathscr{L}_D^*$, explicitly derived in Sec. IVD, is not required for the present argument. Substituting $\mathbf{P_x}$, $\mathbf{P_y}$, and $\mathbf{P_z}$ for $\mathbf{X}$ would yield the GBE.

The connection to thermodynamics is established by examining the energy flow in the problem. Selecting from the total Hamiltonian, Eq. (2.2), the terms that depend only on the TLS degrees of freedom, one is left with $\mathbf{H_s^0}+\mathbf{W}(t)$, which is the total energy of the TLS. Substituting $\mathbf{H_s}\equiv\mathbf{H_s^0}+\mathbf{W}(t)$ for $\mathbf{X}$ in Eq. (3.1) leads to the equation of motion for the TLS energy operator:

$$\frac{d\mathbf{H_s}}{dt}=\frac{\partial\mathbf{W}}{\partial t}+\mathscr{L}_D^*(\mathbf{H_s}). \tag{3.2}$$

The expectation value of Eq. (3.2) becomes the time derivative of the first law of thermodynamics. $\langle\partial\mathbf{W}/\partial t\rangle$ corresponds to the energy flow due to the interaction with the driving field, i.e. to the rate of work performed on the TLS by the field. The latter is simply the power, $\mathscr{P}$:

$$\mathscr{P}=\left\langle\frac{\partial\mathbf{W}}{\partial t}\right\rangle=2\epsilon\omega[-\langle\mathbf{P_x}\rangle\,\sin(\omega t)+\langle\mathbf{P_y}\rangle\,\cos(\omega t)]. \tag{3.3}$$

$\langle\mathscr{L}_D^*(\mathbf{H_s})\rangle$ corresponds to the energy flow due to the interaction with the heat bath, i.e. to the rate of heat flow:

$$\dot{Q}=\langle\mathscr{L}_D^*(\mathbf{H_s})\rangle. \tag{3.4}$$

Eqs. (3.3) and (3.4) constitute the essential link between quantum observables and the thermodynamical path functions.

The TLS in this setup will never reach a state of thermal equilibrium due to the constant flow of energy from the field. Hence, there is no advantage to using state functions and it becomes natural to work with the path functions of heat and work. The TLS approaches a steady state when the energy flows are balanced, i.e. the power from the driving field and the heat flow from the bath balance each other. Applying the first law of thermodynamics, Eq. (3.2), in steady state, implies that $\mathscr{P}^{ss}=-\dot{Q}^{ss}$. However, both directions of energy flow are allowed by the first law: from the driving field to the bath and vice versa. Yet, the second law of thermodynamics asserts that one can only turn work into heat, but not the other way around. In spectroscopic terms this statement implies that a steady-state stimulated *emission* spectra from a TLS immersed in a positive temperature heat bath is *not* allowed. Hence, in steady state $\mathscr{P}$ has to be positive and the heat flow $\dot{Q}$ negative. A thermodynamically consistent theory should comply with this constraint.

IV. DERIVATION OF GENERALIZED BLOCH EQUATIONS

The goal is to derive a consistent set of equations of motion for the TLS observables, based on the assumptions of weak coupling to the bath ($\delta\ll1$), for an unrestricted field intensity (i.e., arbitrary ϵ). The derivation also assumes that the time scale of the relaxation of the TLS is much slower than that associated with the decay of the bath correlation functions and the period of the field ($2\pi\omega^{-1}$).

A schematic outline of the steps in the derivation is as follows:

(a) Transformation to the rotating frame, where the explicit time dependence in $\mathbf{H}$ is transferred from the field-TLS interaction term $\mathbf{W}$ into the TLS-bath interaction term $\mathbf{H_{bs}}$.

(b) Diagonalization of the time-independent effective TLS Hamiltonian in the rotating frame and expressing the total Hamiltonian in terms of projectors in the new diagonalized representation.

(c) Transformation to the interaction picture by using the sum of the time-independent effective TLS Hamiltonian and the free bath Hamiltonian ($\mathbf{H_b}$).

(d) Perturbation expansion to second order in the coupling to the bath, δ, providing an approximate Liouville equation for the extended system (i.e. bath+TLS).

(e) Reduction by performing a partial trace over the degrees of freedom of the bath. This is supplemented by the assumption of a tensor product initial density operator of the extended system, with the bath in thermal equilibrium with respect to its free Hamiltonian, $\mathbf{H_b}$.

(f) Separation of time scales by assuming that the bath fluctuations decay much faster than the TLS relaxation.

(g) Neglect of terms rotating at once or twice the field's frequency.

(h) Transformation of the equations from the rotating-Schrödinger picture to the Heisenberg picture, and evaluation of the GBE in the representation diagonal in the effective TLS Hamiltonian in the rotating frame.

(i) Presentation of the GBE in terms of the longitudinal polarization and the polarization components in and out of phase with the rotating field. The final result is presented in Eq. (4.34). The details of the derivation are important in establishing the range of validity of different limits.

Except for steps (a), (b), and (g) the derivation is similar to that of the SBE for systems not subject to time-dependent fields.[1–6,9,11–17] This is basically the spirit of this approach, which allows for the incorporation of the concepts and tools of standard field-free relaxation theory into the present problem, once the transformation to the rotating frame is accomplished.

A. Transformation to the rotating frame

The density operator of the extended system in the rotating frame, $\hat{\rho}$, is defined by:

$$\hat{\rho}(t)=e^{i\omega\mathbf{P_z}t}\rho(t)e^{-i\omega\mathbf{P_z}t}. \tag{4.1}$$

The Liouville equation in the rotating frame, generating the dynamics of $\hat{\rho}$, is given by

$$\frac{\partial\hat{\rho}}{\partial t}=-i[\hat{\mathbf{H}}(t),\hat{\rho}]\equiv-i\hat{\mathscr{L}}(t)\hat{\rho}, \tag{4.2}$$

where,

$$\hat{\mathbf{H}}=e^{i\omega\mathbf{P_z}t}\mathbf{H}e^{-i\omega\mathbf{P_z}t}=\mathbf{H_b}+\hat{\mathbf{H}}_\mathbf{s}+\hat{\mathbf{H}}_\mathbf{bs}, \tag{4.3}$$

$$\hat{\mathbf{H}}_\mathbf{s}=\Delta\omega\mathbf{P_z}+\epsilon(\mathbf{P_+}+\mathbf{P_-}),\quad \Delta\omega=\omega_0-\omega, \tag{4.4}$$

$$\hat{\mathbf{H}}_\mathbf{bs}=\delta\{e^{i\omega t}\mathbf{\Lambda}\otimes\mathbf{P_+}+e^{-i\omega t}\mathbf{\Lambda}^\dagger\otimes\mathbf{P_-}+\mathbf{\Delta}\otimes\mathbf{P_z}\}. \tag{4.5}$$

$\Delta\omega$ in Eq. (4.4) is usually referred to as the detuning. A geometrical interpretation of the transformation to the rotating frame is shown in Fig. 2.

The effective total Hamiltonian, $\hat{\mathbf{H}}$ [cf. Eq. (4.3)], is divided into three contributions: (a) the original free bath Hamiltonian, $\mathbf{H_b}$; (b) an effective time-independent free TLS Hamiltonian, $\hat{\mathbf{H}}_\mathbf{s}$, which combines the contributions of $\mathbf{H_s^0}$ and $\mathbf{W}$ from the original Hamiltonian; and (c) an explicitly time-dependent TLS-bath interaction Hamiltonian, $\hat{\mathbf{H}}_\mathbf{bs}$.

This structure is similar to that encountered in field-free relaxation theory.[1–6,9,11–17] However, three differences can be noticed.

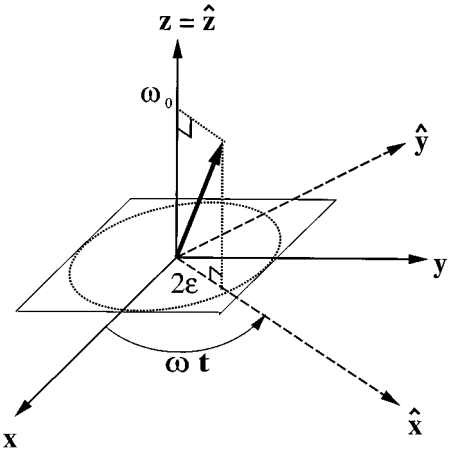

FIG. 2. A geometrical representation of the Hamiltonian $\mathbf{H_s^0}+\mathbf{W}(t)$. The total field is shown as seen in the *stationary* frame, i.e. with longitudinal component ω_0 and rotating transverse component 2ϵ. The reference frame *rotating* with the transverse field is also shown. Note that the $\hat{x}$ axis coincides with the rotating transverse component.

(1) $\hat{\mathbf{H}}$ in Eq. (4.3) is the effective Hamiltonian in the rotating frame. In the field-free theory the original Hamiltonian already has this structure, since $\mathbf{W}=0$.

(2) The TLS-bath interaction Hamiltonian in the rotating frame is explicitly time-dependent, and contains terms that oscillate with the field.

(3) $\hat{\mathbf{H}}_\mathbf{bs}$ is not given in terms of the eigen-projectors of $\hat{\mathbf{H}}_\mathbf{s}$ (whereas $\mathbf{H_{bs}}$ is given in terms of the eigen-projectors of $\mathbf{H_s^0}$).

B. Transformation to the eigen-representation of $\hat{\mathbf{H}}_\mathbf{s}$

To derive the GBE it proves very convenient to transform to the eigen-representation of $\hat{\mathbf{H}}_\mathbf{s}$. In this representation

$$\hat{\mathbf{H}}_\mathbf{s}=\nu\mathbf{\Pi_z} \tag{4.6}$$

and

$$\hat{\mathbf{H}}_\mathbf{bs}=\delta\{\hat{\mathscr{G}}(t)\otimes\mathbf{\Pi_+}+\hat{\mathscr{G}}^\dagger(t)\otimes\mathbf{\Pi_-}+\hat{\mathscr{L}}(t)\otimes\mathbf{\Pi_z}\}, \tag{4.7}$$

where

$$\nu=\sqrt{(\Delta\omega)^2+(2\epsilon)^2}, \tag{4.8}$$

$$\begin{pmatrix}\mathbf{\Pi_+}\\ \mathbf{\Pi_-}\\ \mathbf{\Pi_z}\end{pmatrix}=\begin{pmatrix}\cos^2(\theta/2) & -\sin^2(\theta/2) & -\sin(\theta)\\ -\sin^2(\theta/2) & \cos^2(\theta/2) & -\sin(\theta)\\ \frac{1}{2}\sin(\theta) & \frac{1}{2}\sin(\theta) & \cos(\theta)\end{pmatrix}\begin{pmatrix}\mathbf{P_+}\\ \mathbf{P_-}\\ \mathbf{P_z}\end{pmatrix}, \tag{4.9}$$

$$\begin{pmatrix} \hat{\mathscr{G}}(t) \\ \hat{\mathscr{G}}^{\dagger}(t) \\ \hat{\mathscr{D}}(t) \end{pmatrix}$$

$$= \begin{pmatrix} \cos^2(\theta/2)e^{i\omega t} & -\sin^2(\theta/2)e^{-i\omega t} & -\frac{1}{2}\sin(\theta) \\ -\sin^2(\theta/2)e^{i\omega t} & \cos^2(\theta/2)e^{-i\omega t} & -\frac{1}{2}\sin(\theta) \\ \sin(\theta)e^{i\omega t} & \sin(\theta)e^{-i\omega t} & \cos(\theta) \end{pmatrix}$$

$$\times \begin{pmatrix} \mathbf{\Lambda} \\ \mathbf{\Lambda}^{\dagger} \\ \mathbf{\Delta} \end{pmatrix}, \tag{4.10}$$

and

$$\tan(\theta) = \frac{2\epsilon}{\Delta\omega}. \tag{4.11}$$

ν is the magnitude of the effective field in the rotating frame. It reduces to the Rabi frequency, 2ϵ, in resonance. ν will be referred to as the ''generalized Rabi frequency'' in what follows. A geometrical interpretation of this transformation is shown in Fig. 3.

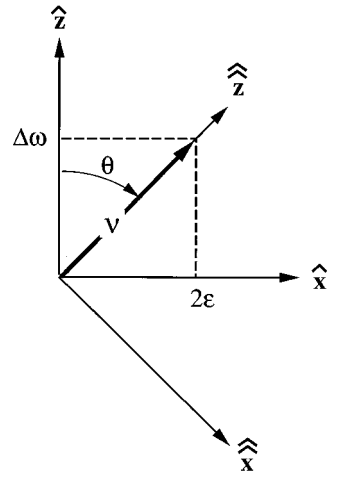

FIG. 3. A geometrical interpretation of the transformation to the eigenrepresentation of $\hat{\mathbf{H}}_s$. The latter is analogous to a transformation to a reference frame rotated by θ around the $\hat{y}$ axis of the rotating frame. Note that both $(\hat{x},\hat{y},\hat{z})$ and $(\hat{\hat{x}},\hat{\hat{y}},\hat{\hat{z}})$ are rotating frames.

C. Transformation to the interaction picture

The next step is a transformation to the interaction picture. The general strategy is similar to that in the absence of the field. The effective Hamiltonian of the extended system, $\hat{\mathbf{H}}$, is divided into a time-independent zero-order Hamiltonian and an explicitly time-dependent perturbation:

$$\hat{\mathbf{H}} = \hat{\mathbf{H}}_0 + \hat{\mathbf{H}}_{bs}, \tag{4.12}$$

where

$$\hat{\mathbf{H}}_0 = \mathbf{H}_b + \hat{\mathbf{H}}_s. \tag{4.13}$$

Based on this partition, a transformation to an ''interaction picture'' is performed by moving $\hat{\rho}(t)$ backward in time using only $\hat{\mathbf{H}}_0$. Note that this interaction picture is defined with respect to the rotating frame.

Actually, the sequence of transformations, first to the rotating frame and then to the interaction picture with respect to the rotating frame, is equivalent to a single transformation to an interaction picture with the time-dependent zero-order Hamiltonian $\mathbf{H}_0 = \mathbf{H}_b + \mathbf{H}_s^0 + \mathbf{W}(t)$.[19] In the special case of the rotating field, this transformation is possible even though the zero-order Hamiltonian is explicitly time-dependent, and the above mentioned sequence of transformations is an effective means to actually carry it out. The same transformation is much less amenable to an analytical treatment in the case of different types of driving fields.

The density operator of the extended system in the interaction (rotating) picture is given by

$$\tilde{\rho} = e^{i\hat{\mathbf{H}}_0 t}\hat{\rho}e^{-i\hat{\mathbf{H}}_0 t}. \tag{4.14}$$

The Liouville equation for $\tilde{\rho}$ is given by

$$\frac{\partial\tilde{\rho}}{\partial t} = -i[\tilde{\mathbf{H}}_{bs}(t),\tilde{\rho}] = -i\tilde{\mathscr{L}}(t)\tilde{\rho}, \tag{4.15}$$

where

$$\tilde{\mathbf{H}}_{bs}(t) = e^{i\hat{\mathbf{H}}_0 t}\hat{\mathbf{H}}_{bs}e^{-i\hat{\mathbf{H}}_0 t} = \delta\{\tilde{\mathscr{G}}(t)\otimes\mathbf{\Pi}_+ + \tilde{\mathscr{G}}^{\dagger}(t)\otimes\mathbf{\Pi}_- + \tilde{\mathscr{D}}(t)\otimes\mathbf{\Pi}_z\}, \tag{4.16}$$

$$\begin{pmatrix} \tilde{\mathscr{G}}(t) \\ \tilde{\mathscr{G}}^{\dagger}(t) \\ \tilde{\mathscr{D}}(t) \end{pmatrix} = \begin{pmatrix} e^{i(\omega+\nu)t}\cos^2(\theta/2) & -e^{-i(\omega-\nu)t}\sin^2(\theta/2) & -\frac{1}{2}e^{i\nu t}\sin(\theta) \\ -e^{i(\omega-\nu)t}\sin^2(\theta/2) & e^{-i(\omega+\nu)t}\cos^2(\theta/2) & -\frac{1}{2}e^{-i\nu t}\sin(\theta) \\ e^{i\omega t}\sin(\theta) & e^{-i\omega t}\sin(\theta) & \cos(\theta) \end{pmatrix} \begin{pmatrix} \mathbf{\Lambda}(t) \\ \mathbf{\Lambda}^{\dagger}(t) \\ \mathbf{\Delta}(t) \end{pmatrix}, \tag{4.17}$$

and

$$\mathbf{\Lambda}(t)=e^{i\mathbf{H_b}t}\mathbf{\Lambda}e^{-i\mathbf{H_b}t},\quad \mathbf{\Lambda}^{\dagger}(t)=e^{i\mathbf{H_b}t}\mathbf{\Lambda}^{\dagger}e^{-i\mathbf{H_b}t},$$
$$\mathbf{\Delta}(t)=e^{i\mathbf{H_b}t}\mathbf{\Delta}e^{-i\mathbf{H_b}t}. \tag{4.18}$$

As a consistency test, when the field is turned off ($\epsilon=0$), $\tilde{\mathbf{H}}_{\mathbf{bs}}(t)$ reduces to $\tilde{\mathbf{H}}_{\mathbf{bs}}(t)=\delta\{e^{i\omega_0 t}\mathbf{\Lambda}(t)\otimes\mathbf{P_+}+e^{-i\omega_0 t}\mathbf{\Lambda}^{\dagger}(t)\otimes\mathbf{P_-}+\mathbf{\Delta}(t)\otimes\mathbf{P_z}\}$ as it should.

D. Derivation of the quantum master equation

The route from the interaction picture Liouville equation to the quantum master equation is similar to the method of deriving the master equation in the absence of the field. The derivation presented here is similar to that developed in Ref. 16. Therefore only a brief and schematic description of the derivation is provided.

The rotating-field-interaction picture Liouville equation, Eq. (4.15), presents the starting point. It is formally solved via a power series expansion in δ, subject to a tensor product initial state for the extended system:

$$\rho(0)=\rho_b\otimes\sigma(0). \tag{4.19}$$

$\sigma(0)$ is the initial reduced density operator of the TLS, and ρ_b is the density operator of the bath in thermal equilibrium:

$$\rho_b=\frac{e^{-\beta\mathbf{H_b}}}{\mathrm{Tr}_b(e^{-\beta\mathbf{H_b}})}. \tag{4.20}$$

The TLS reduced density operator at $t>0$ in the interaction (rotating) picture is given by

$$\tilde{\sigma}(t)=\mathrm{Tr}_b(\tilde{\rho}(t)). \tag{4.21}$$

Tr_b refers to a partial trace over the bath degrees of freedom.

The state of the TLS at time t, $\tilde{\sigma}(t)$, can be formally related to its initial value, $\tilde{\sigma}(0)$, via

$$\tilde{\sigma}(t)=\Phi(t)\tilde{\sigma}(0). \tag{4.22}$$

This is the integral form of the reduced equation of motion. The differential form is obtained from the integral form in the following manner:

$$\frac{d}{dt}\tilde{\sigma}(t)=\dot{\Phi}(t)\tilde{\sigma}(0)=\dot{\Phi}(t)\Phi^{-1}(t)\tilde{\sigma}(t)\equiv\mathbf{R}(t)\tilde{\sigma}(t). \tag{4.23}$$

The generator $\mathbf{R}(t)$ is then expanded in powers of δ. This expansion is truncated at second order in δ, thereby introducing the assumption of weak coupling to the heat bath. The first order term in δ vanishes on account of the original definition of the bath operators (recall that $\langle\mathbf{\Lambda}\rangle_b=\langle\mathbf{\Lambda}^{\dagger}\rangle_b=\langle\mathbf{\Delta}\rangle_b=0$).

After truncation at second order in δ, and subsequently setting $\delta=1$ (from this point on we will assume that $\mathbf{\Lambda}$ and $\mathbf{\Delta}$ are appropriately "small"), the reduced equation of motion becomes

$$\begin{aligned}\frac{d}{dt}\tilde{\sigma}=&-\int_0^t dt_1\mathrm{Tr}_b(\tilde{\mathscr{L}}(t)\tilde{\mathscr{L}}(t_1)\rho_b)\tilde{\sigma}=\int_0^t dt_1\{\mathrm{Tr}_b(\tilde{\mathscr{G}}(t)\tilde{\mathscr{G}}(t_1)\rho_b)\}[\Pi_+,\Pi_+\tilde{\sigma}]+\text{h.c.}\\
&-\int_0^t dt_1\{\mathrm{Tr}_b(\tilde{\mathscr{G}}(t)\tilde{\mathscr{G}}^{\dagger}(t_1)\rho_b)\}[\Pi_+,\Pi_-\tilde{\sigma}]+\text{h.c.}-\int_0^t dt_1\{\mathrm{Tr}_b(\tilde{\mathscr{G}}(t)\tilde{\mathscr{L}}(t_1)\rho_b)\}[\Pi_+,\Pi_z\tilde{\sigma}]+\text{h.c.}\\
&-\int_0^t dt_1\{\mathrm{Tr}_b(\tilde{\mathscr{G}}^{\dagger}(t)\tilde{\mathscr{G}}(t_1)\rho_b)\}[\Pi_-,\Pi_+\tilde{\sigma}]+\text{h.c.}-\int_0^t dt_1\{\mathrm{Tr}_b(\tilde{\mathscr{G}}^{\dagger}(t)\tilde{\mathscr{G}}^{\dagger}(t_1)\rho_b)\}[\Pi_-,\Pi_-\tilde{\sigma}]+\text{h.c.}\\
&-\int_0^t dt_1\{\mathrm{Tr}_b(\tilde{\mathscr{G}}^{\dagger}(t)\tilde{\mathscr{L}}(t_1)\rho_b)\}[\Pi_-,\Pi_z\tilde{\sigma}]+\text{h.c.}-\int_0^t dt_1\{\mathrm{Tr}_b(\tilde{\mathscr{L}}(t)\tilde{\mathscr{G}}(t_1)\rho_b)\}[\Pi_z,\Pi_+\tilde{\sigma}]+\text{h.c.}\\
&-\int_0^t dt_1\{\mathrm{Tr}_b(\tilde{\mathscr{L}}(t)\tilde{\mathscr{G}}^{\dagger}(t_1)\rho_b)\}[\Pi_z,\Pi_-\tilde{\sigma}]+\text{h.c.}-\int_0^t dt_1\{\mathrm{Tr}_b(\tilde{\mathscr{L}}(t)\tilde{\mathscr{L}}(t_1)\rho_b)\}[\Pi_z,\Pi_z\tilde{\sigma}]+\text{h.c.},\end{aligned} \tag{4.24}$$

where h.c. corresponds to Hermitian conjugate of the preceding term.

Each of the 18 terms on the rhs of Eq. (4.24) is a product of two factors. The first factor is an integral over a trace involving only bath operators. The second factor is a commutator involving only TLS operators. In order to conclude the derivation, the bath factors are evaluated explicitly. The evaluation of the bath factors is demonstrated in some detail for the first term in Appendix A. The other bath factors may be evaluated in a similar manner.

The evaluation of the bath factors involves three major assumptions or approximations.

(a) The decay of the bath correlation functions is very fast on the time-scale of the TLS relaxation. Therefore the validity of the equations is limited to the description of the dynamics for time-scales long compared to that associated with the decay of the bath correlation functions. Note that this assumption of time-scale separation is completely consistent with the weak-coupling limit in that in this limit the TLS relaxation rate constants are arbitrarily small.

(b) Terms rotating like $e^{\pm i\omega t}$ or $e^{\pm 2i\omega t}$ can be neglected. This is a valid approximation if the frequency of the field is fast on the time-scale of the TLS relaxation. A very important consequence of this approximation is that the only re-

maining bath correlation functions are $C_{\Lambda\Lambda^\dagger}(\tau)$, $C_{\Lambda^\dagger\Lambda}(\tau)$, and $C_{\Delta\Delta}(\tau)$, where

$$C_{AB}(\tau)=\mathrm{Tr}_b(A(\tau)B\rho_b) \tag{4.25}$$

(cf. Appendix A).

(c) The bath factors turn out to be complex. The imaginary part contributes to the oscillatory Hamiltonian dynamics, while the real part introduces a genuine non-oscillatory contribution into the overall dynamics, leading to relaxation. The third approximation is introduced by neglecting the imaginary part of the bath factor. This means that the bath-induced Hamiltonian dynamics is negligible in comparison with that induced by $\hat{\mathbf{H}}_\mathbf{s}$.

Once evaluated by incorporating the above approximations, all bath factors turn into (except for trivial oscillatory factors) real and positive time-independent rate coefficients denoted by γ_1, γ_2, $\gamma_3 \ldots \gamma_9$ according to their order of appearance in Eq. (4.24). Note that each term and its Hermitian conjugate share the same rate coefficient. These rate coefficients are explicitly given in Appendix B.

For ease of interpretation the master equation is transformed into the Heisenberg picture. This transformation is described in detail in Appendix C. The Heisenberg equation of motion for a TLS observable, $\mathbf{X}$, is then given by

$$\begin{aligned}\frac{d}{dt}\mathbf{X}=&i[\mathbf{H_s^0}+\mathbf{W}(t),\mathbf{X}]+\frac{\partial\mathbf{X}}{\partial t}-\gamma_1\{[\mathbf{X},\hat{\mathbf{\Pi}}_+]\hat{\mathbf{\Pi}}_+ +\hat{\mathbf{\Pi}}_-[\hat{\mathbf{\Pi}}_-,\mathbf{X}]\}-\gamma_2\{[\mathbf{X},\hat{\mathbf{\Pi}}_+]\hat{\mathbf{\Pi}}_- +\hat{\mathbf{\Pi}}_+[\hat{\mathbf{\Pi}}_-,\mathbf{X}]\}\\ &-\gamma_3\{[\mathbf{X},\hat{\mathbf{\Pi}}_+]\hat{\mathbf{\Pi}}_z+\hat{\mathbf{\Pi}}_z[\hat{\mathbf{\Pi}}_-,\mathbf{X}]\}-\gamma_4\{[\mathbf{X},\hat{\mathbf{\Pi}}_-]\hat{\mathbf{\Pi}}_+ +\hat{\mathbf{\Pi}}_-[\hat{\mathbf{\Pi}}_+,\mathbf{X}]\}-\gamma_5\{[\mathbf{X},\hat{\mathbf{\Pi}}_-]\hat{\mathbf{\Pi}}_- +\hat{\mathbf{\Pi}}_+[\hat{\mathbf{\Pi}}_+,\mathbf{X}]\}\\ &-\gamma_6\{[\mathbf{X},\hat{\mathbf{\Pi}}_-]\hat{\mathbf{\Pi}}_z+\hat{\mathbf{\Pi}}_z[\hat{\mathbf{\Pi}}_+,\mathbf{X}]\}-\gamma_7\{[\mathbf{X},\hat{\mathbf{\Pi}}_z]\hat{\mathbf{\Pi}}_+ +\hat{\mathbf{\Pi}}_-[\hat{\mathbf{\Pi}}_z,\mathbf{X}]\}\\ &-\gamma_8\{[\mathbf{X},\hat{\mathbf{\Pi}}_z]\hat{\mathbf{\Pi}}_- +\hat{\mathbf{\Pi}}_+[\hat{\mathbf{\Pi}}_z,\mathbf{X}]\}-\gamma_9\{[\mathbf{X},\hat{\mathbf{\Pi}}_z]\hat{\mathbf{\Pi}}_z+\hat{\mathbf{\Pi}}_z[\hat{\mathbf{\Pi}}_z,\mathbf{X}]\}.\end{aligned} \tag{4.26}$$

It should be noted that Eq. (4.26) corresponds to the regular Heisenberg picture. Hence, the observable $\mathbf{X}$ should be defined with respect to the *stationary* frame of reference. The operators $\hat{\mathbf{\Pi}}_+$, $\hat{\mathbf{\Pi}}_-$, and $\hat{\mathbf{\Pi}}_z$ are explicitly time-dependent. They are related to the original operators by the transformation

$$\begin{pmatrix}\hat{\mathbf{\Pi}}_+\\ \hat{\mathbf{\Pi}}_-\\ \hat{\mathbf{\Pi}}_z\end{pmatrix}=\begin{pmatrix}\cos^2(\theta/2)e^{-i\omega t} & -\sin^2(\theta/2)e^{i\omega t} & -\sin(\theta)\\ -\sin^2(\theta/2)e^{-i\omega t} & \cos^2(\theta/2)e^{i\omega t} & -\sin(\theta)\\ \frac{1}{2}e^{-i\omega t}\sin(\theta) & \frac{1}{2}e^{i\omega t}\sin(\theta) & \cos(\theta)\end{pmatrix}\times\begin{pmatrix}\mathbf{P_+}\\ \mathbf{P_-}\\ \mathbf{P_z}\end{pmatrix}. \tag{4.27}$$

Therefore the dynamics of the TLS is completely governed by the change of the other three operators, or their expectation values. These three equations of motion constitute the GBE.

Since the specific set of three independent operators is rather arbitrary, the choice is a matter of convenience. Also, once stated in terms of one set of operators, the GBE can always be transformed into another set. Most of the effort involved in the evaluation of the GBE has to do with the evaluation of the dissipation super-operator in the quantum master equation, Eq. (4.26). Since the latter is given in terms of the operators $\hat{\mathbf{\Pi}}_+$, $\hat{\mathbf{\Pi}}_-$, and $\hat{\mathbf{\Pi}}_z$, which constitute an independent set, it is most convenient to first evaluate the GBE in terms of these operators, and later transform to other sets if the need arises. For ease of interpretation a set of Hermitian operators is advantageous. Hence, after obtaining the equations in terms of $\hat{\mathbf{\Pi}}_+$, $\hat{\mathbf{\Pi}}_-$, and $\hat{\mathbf{\Pi}}_z$ they are transformed to the set $\hat{\mathbf{\Pi}}_x$, $\hat{\mathbf{\Pi}}_y$, and $\hat{\mathbf{\Pi}}_z$, where the Hermitian $\hat{\mathbf{\Pi}}_x$ and $\hat{\mathbf{\Pi}}_y$ are the following linear combinations of $\hat{\mathbf{\Pi}}_+$ and $\hat{\mathbf{\Pi}}_-$:

$$\hat{\mathbf{\Pi}}_x=\tfrac{1}{2}(\hat{\mathbf{\Pi}}_+ +\hat{\mathbf{\Pi}}_-),\quad \hat{\mathbf{\Pi}}_y=\frac{1}{2i}(\hat{\mathbf{\Pi}}_+ -\hat{\mathbf{\Pi}}_-). \tag{4.28}$$

The operators $\hat{\mathbf{\Pi}}_x$, $\hat{\mathbf{\Pi}}_y$ and $\hat{\mathbf{\Pi}}_z$ have a straightforward geometrical interpretation as polarization components along the axes of the $(\hat{x},\hat{y},\hat{z})$ rotating frame (cf. Fig. 3). This choice of observables is referred as "the Π representation."

The GBE in the Π representation are given by

E. The generalized Bloch equations (GBE)

The state of the TLS can be expressed by a density operator in a four-dimensional Hilbert-Schmidt operator space defined by the scalar product $(\mathbf{A}\cdot\mathbf{B})=\mathrm{Tr}\{\mathbf{A}^\dagger\mathbf{B}\}$. The basis of this space consists of four independent operators. One of these operators can be chosen as the identity operator. The other three can be chosen in various ways. The identity operator does not change due to the conservation of probability.

$$\frac{d}{dt}\begin{pmatrix}\hat{\mathbf{\Pi}}_x\\ \hat{\mathbf{\Pi}}_y\\ \hat{\mathbf{\Pi}}_z\end{pmatrix} = \begin{pmatrix}\lambda-(\frac{1}{2}\Gamma_p+\Gamma'_d) & -\nu & \eta\\ \nu & -(\lambda+\frac{1}{2}\Gamma_p+\Gamma'_d) & 0\\ 2\xi & 0 & -\Gamma_p\end{pmatrix} \times\begin{pmatrix}\hat{\mathbf{\Pi}}_x\\ \hat{\mathbf{\Pi}}_y\\ \hat{\mathbf{\Pi}}_z\end{pmatrix} - \begin{pmatrix}\alpha\\ 0\\ \delta\end{pmatrix}, \tag{4.29}$$

where,

$$\begin{aligned}\Gamma_p &= 2(\gamma_2+\gamma_4),\\ \Gamma'_d &= \gamma_9,\\ \lambda &= \gamma_1+\gamma_5,\\ \eta &= \gamma_7+\gamma_8,\\ \xi &= \tfrac{1}{2}(\gamma_3+\gamma_6),\\ \alpha &= \tfrac{1}{2}(\gamma_6-\gamma_3+\gamma_7-\gamma_8),\\ \delta &= \gamma_2-\gamma_4.\end{aligned} \tag{4.30}$$

(The explicit expressions for $\gamma_1 \ldots \gamma_9$ are given in Appendix B.)

It is convenient to write the relaxation coefficients in terms of the following four functions:

$$\begin{aligned}\Gamma^0_p(x) &\equiv \tilde{C}_{\Lambda\Lambda^\dagger}(x)(1+e^{-\beta x}),\\ \Gamma'^0_d(x) &\equiv \tfrac{1}{4}\tilde{C}_{\Delta\Delta}(x)(1+e^{-\beta x}),\\ \delta^0(x) &\equiv \tfrac{1}{2}\tilde{C}_{\Lambda\Lambda^\dagger}(x)(1-e^{-\beta x}),\\ \alpha^0(x) &= \tfrac{1}{4}\tilde{C}_{\Delta\Delta}(x)(1-e^{-\beta x}),\end{aligned} \tag{4.31}$$

where $\tilde{C}_{AB}(x)$ is the Fourier transform of $C_{AB}(t)$, as defined in Appendix A. The significance of these definitions arises from the following identities tying these coefficients to the field-free case:

$$\begin{aligned}\Gamma^0_p(\omega_0) &= \frac{1}{T_1},\\ \Gamma'^0_d(0) &= \frac{1}{T'_2},\\ -\frac{\delta^0(\omega_0)}{\Gamma^0_p(\omega_0)} &= -\frac{1}{2}\tanh\left(\frac{\beta\omega_0}{2}\right) \equiv P^{eq}_z,\\ \alpha^0(0) &= 0.\end{aligned} \tag{4.32}$$

T_1 is the field-free time constant for population relaxation, T'_2 is the field-free time constant for pure dephasing, and P^{eq}_z is the field-free thermal equilibrium expectation value of $\mathbf{P_z}$ (the field-free thermal equilibrium expectation values of $\mathbf{P_x}$ and $\mathbf{P_y}$ vanish). The function α^0 is new since it does not appear in the field free case.

TABLE I. The bath coefficients in the Π representation. s and c stand for $\sin(\theta)$ and $\cos(\theta)$, respectively.

	$\Gamma^0_p(\omega-\nu)$	$\Gamma^0_p(\omega)$	$\Gamma^0_p(\omega+\nu)$	$\Gamma'^0_d(0)$	$\Gamma'^0_d(\nu)$
Γ_p	$(1-c)^2/4$	0	$(1+c)^2/4$	0	s^2
Γ'_d	0	$s^2/2$	0	c^2	0
λ	$-s^2/8$	0	$-s^2/8$	0	$s^2/2$
η	$s(c-1)/4$	0	$s(c+1)/4$	0	$-s$
ξ	0	$sc/4$	0	$-sc/2$	0

The coefficients Γ_p, Γ'_d, λ, η and ξ in Eq. (4.29) can be written as linear combinations of $\Gamma^0_p(\omega)$, $\Gamma^0_p(\omega+\nu)$, $\Gamma^0_p(\omega-\nu)$, $\Gamma'^0_d(0)$ and $\Gamma'^0_d(\nu)$. The expansion coefficients in the linear combinations depend upon θ (cf. Eq. (4.11)). Γ_p, Γ'_d, λ, η and ξ, written in this manner, are summarized in Table I. Note that the arguments of Γ^0_p and Γ'^0_d can involve ν, which depends on ϵ, and that θ is also explicitly field-dependent. Hence, the relaxation becomes explicitly field-dependent.

The inhomogeneous terms δ and α in Eq. (4.29) are written as linear combinations of $\delta^0(\omega-\nu)$, $\delta^0(\omega)$, $\delta^0(\omega+\nu)$ and $\alpha^0(\nu)$. As before, the coefficients of these functions depend upon θ. δ and α, written in this manner, are shown in Table II. Note that δ^0 and α^0 have the same arguments as Γ^0_p and Γ'^0_d respectively, and that δ and α are also explicitly field-dependent.

The final form of the GBE is written in terms of yet another set of independent observables: $\hat{\mathbf{P}}_\mathbf{x}$, $\hat{\mathbf{P}}_\mathbf{y}$ and $\hat{\mathbf{P}}_\mathbf{z}$, defined by

$$\begin{aligned}\hat{\mathbf{P}}_\mathbf{x} &= \tfrac{1}{2}(e^{-i\omega t}\mathbf{P}_+ + e^{i\omega t}\mathbf{P}_-) = \mathbf{P_x}\cos(\omega t)+\mathbf{P_y}\sin(\omega t),\\ \hat{\mathbf{P}}_\mathbf{y} &= \frac{1}{2i}(e^{-i\omega t}\mathbf{P}_+ - e^{i\omega t}\mathbf{P}_-) = -\mathbf{P_x}\sin(\omega t)+\mathbf{P_y}\cos(\omega t),\\ \hat{\mathbf{P}}_\mathbf{z} &= \mathbf{P_z}.\end{aligned} \tag{4.33}$$

Equivalent and more familiar notations for $\hat{\mathbf{P}}_\mathbf{x}$, $\hat{\mathbf{P}}_\mathbf{y}$ and $\hat{\mathbf{P}}_\mathbf{z}$ (or more precisely, their expectation values) that were introduced by Bloch[1] are the polarization functions u, v, and w. These observables are the polarization components in a coordinate system rotating with the field. $\hat{\mathbf{P}}_\mathbf{x}$ is the transverse polarization along the direction of the rotating field, $\hat{\mathbf{P}}_\mathbf{y}$ is the transverse polarization out of phase with the rotating field, and $\hat{\mathbf{P}}_\mathbf{z}$ is the longitudinal polarization (cf. Fig. 2). This choice of observable is referred as "the P representation."

The GBE equation in the P representation become

TABLE II. The inhomogeneous terms in the Π representation. s and c stand for $\sin(\theta)$ and $\cos(\theta)$, respectively.

	$\delta^0(\omega-\nu)$	$\delta^0(\omega)$	$\delta^0(\omega+\nu)$	$\alpha^0(\nu)$
α	$s(c-1)/4$	$-s/2$	$-s(c+1)/4$	$sc/2$
δ	$-(1-c)^2/4$	0	$(1+c)^2/4$	$s^2/2$

TABLE III. Relaxation rates in the P representation. s and c stand for $\sin(\theta)$ and $\cos(\theta)$, respectively.

	$\Gamma_p^0(\omega-\nu)$	$\Gamma_p^0(\omega)$	$\Gamma_p^0(\omega+\nu)$	$\Gamma_d'^0(0)$	$\Gamma_d'^0(\nu)$
Γ_x	$(1-c)/4$	0	$(1+c)/4$	c^2	s^2
Γ_y	$c(c-1)/4$	$s^2/2$	$c(c+1)/4$	c^2	s^2
Γ_z	$(1-c)^2/4$	$s^2/2$	$(1+c)^2/4$	0	0
Γ_{xz}	0	0	0	sc	$-sc$
Γ_{zx}	$s(1-c)/4$	$sc/2$	$-s(1+c)/4$	0	0

$$\frac{d}{dt}\begin{pmatrix}\hat{\mathbf{P}}_x\\ \hat{\mathbf{P}}_y\\ \hat{\mathbf{P}}_z\end{pmatrix}=\begin{pmatrix}-\Gamma_x & -\Delta\omega & \Gamma_{xz}\\ \Delta\omega & -\Gamma_y & -2\epsilon\\ \Gamma_{zx} & 2\epsilon & -\Gamma_z\end{pmatrix}\begin{pmatrix}\hat{\mathbf{P}}_\mathbf{x}\\ \hat{\mathbf{P}}_\mathbf{y}\\ \hat{\mathbf{P}}_\mathbf{z}\end{pmatrix}-\begin{pmatrix}\gamma_x\\ 0\\ \gamma_z\end{pmatrix}. \tag{4.34}$$

The relaxation coefficients Γ_x, Γ_y, Γ_z, Γ_{xz}, and Γ_{zx}, and inhomogeneous terms γ_x and γ_z are given explicitly in terms of the functions Γ_p^0, $\Gamma_d'^0$, δ^0 and α^0 in Tables III and IV.

For comparison, the SBE written in terms of the P representation have the following form:

$$\frac{d}{dt}\begin{pmatrix}\hat{\mathbf{P}}_x\\ \hat{\mathbf{P}}_y\\ \hat{\mathbf{P}}_z\end{pmatrix}=\begin{pmatrix}-\frac{1}{T_2} & -\Delta\omega & 0\\ \Delta\omega & -\frac{1}{T_2} & -2\epsilon\\ 0 & 2\epsilon & -\frac{1}{T_1}\end{pmatrix}\begin{pmatrix}\hat{\mathbf{P}}_\mathbf{x}\\ \hat{\mathbf{P}}_\mathbf{y}\\ \hat{\mathbf{P}}_\mathbf{z}\end{pmatrix}+\begin{pmatrix}0\\ 0\\ \frac{P_z^{eq}}{T_1}\end{pmatrix}, \tag{4.35}$$

where

$$\frac{1}{T_2}=\frac{1}{2T_1}+\frac{1}{T_2'}. \tag{4.36}$$

T_1, T_2' and P_z^{eq} were related to $\Gamma_p^0(\omega_0)$, $\Gamma_d'^0(0)$ and $\delta^0(\omega_0)$ in Eq. (4.32).

Comparison of the SBE, Eq. (4.35), with the GBE in the P representation, Eq. (4.34), reveals the following differences:

(1) The relaxation coefficients in the GBE depend explicitly upon the amplitude and frequency of the field. The corresponding coefficients in the SBE are field-independent.

(2) The relaxation rates of $\hat{\mathbf{P}}_\mathbf{x}$ and $\hat{\mathbf{P}}_\mathbf{y}$ differ in the GBE (i.e. $\Gamma_x \neq \Gamma_y$), whereas in the SBE, $\hat{\mathbf{P}}_\mathbf{x}$ and $\hat{\mathbf{P}}_\mathbf{y}$ share the same relaxation time-constant, T_2. This difference arises from the fact that $\hat{\mathbf{P}}_\mathbf{x}$ is the polarization along the direction of the driving field whereas $\hat{\mathbf{P}}_\mathbf{y}$ is the polarization out of phase with respect to it. Thus, the driving field introduces a physical distinction between the two directions in space and their associated relaxation times, in much the same way that the d.c. field provides a distinctive spatial "z axis" in magnetic resonance, leading to different longitudinal and transverse relaxation times.

(3) Additional off-diagonal relaxation coefficients, Γ_{xz} and Γ_{zx}, appear in the GBE. The physical significance of the rotating xz plane is due to the fact that the total field lies within it. This results in extra coupling terms between the polarization components that lie along the directions of the field.

(4) There is an extra inhomogeneous term in the generalized Bloch equation for $\hat{\mathbf{P}}_\mathbf{x}$, namely γ_x. This is due to the existence of a non-negligible driving field in this direction.

TABLE IV. Inhomogeneous terms in the P representation. s and c stand for $\sin(\theta)$ and $\cos(\theta)$ respectively.

	$\delta^0(\omega-\nu)$	$\delta^0(\omega)$	$\delta^0(\omega+\nu)$	$\alpha^0(\nu)$
γ_x	$s(c-1)/4$	$-sc/2$	$s(c+1)/4$	s/2
γ_z	$(1-c)^2/4$	$s^2/2$	$(1+c)^2/4$	0

V. SPECIAL LIMITS OF THE GENERALIZED BLOCH EQUATIONS

The asymptotic limits where the GBE are reduced to the SBE, or to the generalized optical Bloch equations are examined. These limits depend on the relative magnitudes of the following six frequencies (or energies): 2ϵ (the Rabi frequency), $\Delta\omega$ (the detuning), ν (the generalized Rabi frequency), ω_0 (the TLS frequency), T (the temperature), and $1/\tau_c$ (the inverse correlation time of the diagonal bath fluctuations, to be defined below).

First consider the limit $|2\epsilon| \ll |\Delta\omega|$. In this case, $\nu \approx |\Delta\omega|$, $\sin(\theta)\approx 0$, and $\cos(\theta)$ approaches $+1$ or -1, corresponding to $\Delta\omega$ being positive or negative respectively. If these approximations are implemented into the GBE in the P representation, they reduce to the SBE. Hence, the SBE still hold for considerable field intensities, as long as the field frequency is far enough from resonance. Such a behaviour is expected since tuning the field frequency out of resonance is equivalent to quenching the driving field, and is often used this way.

Next consider the limit $|2\epsilon|, |\Delta\omega| \ll \omega_0, 1/\tau_c$. (For example, this situation is often obtained for electronic transitions, where ω_0 is in the optical regime.) This limit implies that $\nu \ll \omega_0 \approx \omega$, and hence $\Gamma_p^0(\omega), \Gamma_p^0(\omega\pm\nu) \approx \Gamma_p^0(\omega_0)$, and $\delta^0(\omega), \delta^0(\omega\pm\nu) \approx \delta^0(\omega_0)$. Now the coefficients $\Gamma_d'^0(\nu)$ and $\alpha^0(\nu)$ are examined in this limit. These coefficients have the general form:

$$\Gamma_d'^0(\nu) \equiv \tfrac{1}{4}\tilde{C}_{\Delta\Delta}(\nu)(1+e^{-\beta\nu}),$$
$$\alpha^0(\nu) \equiv \tfrac{1}{4}\tilde{C}_{\Delta\Delta}(\nu)(1-e^{-\beta\nu}). \tag{5.1}$$

Note that $\exp(-\beta\nu)\approx 1$ if $\nu \ll T$. The other term in Eq. (5.1), $\tilde{C}_{\Delta\Delta}(\nu)$, is the Fourier transform of the time-correlation function $C_{\Delta\Delta}(\tau)$:

$$\tilde{C}_{\Delta\Delta}(\nu)=\int_{-\infty}^{\infty} d\tau e^{i\nu\tau} C_{\Delta\Delta}(\tau). \tag{5.2}$$

Define the time-scale associated with the decay of $C_{\Delta\Delta}(\tau)$ as τ_c. Since $\nu \ll 1/\tau_c$, i.e. the generalized Rabi frequency is very slow on the time-scale of the decay of the bath fluctuations, $C_{\Delta\Delta}(\tau)$ decays to zero before $\nu\tau$ can change appreciably from its value at $\tau=0$, which is 0. Hence, in this case $\tilde{C}_{\Delta\Delta}(\nu)\approx\tilde{C}_{\Delta\Delta}(0)$. It should be noted that $1/\tau_c$ is of the order of magnitude of the smaller of the two quantities, the bath band width or the temperature T. Hence $\nu \ll 1/\tau_c$ implies that

$\nu \ll T$. Therefore $\Gamma_d'^0(\nu) \approx \Gamma_d'^0(0)$ and $\alpha^0(\nu) \approx 0$. Implementing these approximations into the GBE in the P representation reduces them once more to the SBE (for arbitrary θ). Thus, the above two special cases show that, quite generally, for weak fields the SBE are valid, which is a statement that has been disputed by several authors.[30,31]

Next consider the less restrictive limit $\nu \ll \omega_0$. It is still true that $\Gamma_p^0(\omega), \Gamma_p^0(\omega \pm \nu) \approx \Gamma_p^0(\omega_0)$, and $\delta^0(\omega), \delta^0(\omega \pm \nu) \approx \delta^0(\omega_0)$, but now we have the possibility that ν is on the order of $1/\tau_c$, and so $\Gamma_d'^0(\nu)$ must be kept distinct from $\Gamma_d'^0(0)$, and $\alpha^0(\nu)$ does not vanish. The relaxation coefficients in the P representation then reduce to

$$\begin{aligned}
&\Gamma_x \approx \Gamma_y = \frac{1}{2T_1} + \frac{1}{\nu^2}\left[(\Delta\omega)^2 \Gamma_d'^0(0) + (2\epsilon)^2 \Gamma_d'^0(\nu)\right], \\
&\Gamma_z \approx \frac{1}{T_1}, \\
&\Gamma_{xz} \approx \frac{2\epsilon\Delta\omega}{\nu^2}\left[\Gamma_d'^0(0) - \Gamma_d'^0(\nu)\right], \\
&\Gamma_{zx} \approx 0, \\
&\gamma_x \approx \frac{\epsilon}{\nu}\,\alpha^0(\nu), \\
&\gamma_z \approx \delta^0(\omega_0).
\end{aligned} \tag{5.3}$$

As a result, the coefficients associated with population relaxation remain equal to the coefficients in the SBE. However, the rate of pure dephasing is explicitly field dependent, and furthermore, Γ_{xz} and γ_x do not vanish.

Now consider an additional restriction, such that $\nu \ll \omega_0, T$. If the temperature is *sufficiently* high, then the imaginary part of $C_{\Delta\Delta}(\tau)$ can be neglected in comparison with the real part, and since the real part is even in τ, Eq. (5.3) is valid with

$$\Gamma_d'^0(x) = \int_0^\infty d\tau\, \cos(x\tau)\,\mathrm{Re}[C_{\Delta\Delta}(\tau)], \tag{5.4}$$

and $\gamma_x \approx 0$. In this limit our results are nearly identical to the generalized optical Bloch equations of Yamanoi[28] and Yamanoi and Eberly,[29] who considered a stochastic model of bath fluctuations. The only difference between our results and theirs is that we have neglected a small correction to the Rabi frequency (a correction to Hamiltonian dynamics, as discussed in Appendix A), which appears in the paper by Yamanoi and Eberly as a damping coefficient Γ_{23}. If one further assumes that

$$C_{\Delta\Delta}(\tau) = (\delta\omega)^2 e^{-|\tau|/\tau_c}, \tag{5.5}$$

then the results of Schenzle *et al.*,[30] Berman and Brewer,[32] and Yamanoi and Eberly[34] are recovered.

Next consider the limit $1/\tau_c \ll \nu \ll \omega_0$. In this case $\exp(i\nu\tau)$ oscillates many times before $C_{\Delta\Delta}(\tau)$ can change appreciably. Hence, $\tilde{C}_{\Delta\Delta}(\nu)$ is approximately zero in such a case. The relaxation coefficients in the P representation then reduce to:

$$\begin{aligned}
&\Gamma_x \approx \Gamma_y = \frac{1}{2T_1} + \frac{(\Delta\omega)^2}{(\Delta\omega)^2 + (2\epsilon)^2}\,\frac{1}{T_2'}, \\
&\Gamma_z \approx \frac{1}{T_1}, \\
&\Gamma_{xz} \approx \frac{2\epsilon\Delta\omega}{(\Delta\omega)^2 + (2\epsilon)^2}\,\frac{1}{T_2'}, \\
&\gamma_x \approx 0, \\
&\Gamma_{zx} \approx 0, \\
&\gamma_z \approx \delta^0(\omega_0).
\end{aligned} \tag{5.6}$$

An interesting extreme case of this limit is obtained when $|2\epsilon| \gg |\Delta\omega|$. This case is obtained either by increasing the intensity of the field or by tuning the frequency closer to resonance, which effectively leads to the same result. The GBE reduce in this extreme to the form of the SBE, but with a modified dephasing rate $\Gamma_x = \Gamma_y = 1/2T_1$, rather than $\Gamma_x = \Gamma_y = 1/2T_1 + 1/T_2'$, as in the SBE. Hence pure dephasing is seen to be quenched by the driving field when $|2\epsilon| \gg |\Delta\omega|, 1/\tau_c$. This limit is obtainable for electronic transitions, and indeed, arguments of this sort were used to explain deviations from the SBE in the free-induction decay of $\mathbf{Pr^{3+}}$ in $\mathbf{LaF_3}$.[23]

Finally, consider the near-resonance limit $|\Delta\omega| \ll |2\epsilon|$, with $|2\epsilon|/\omega_0$ arbitrary. Comparable values for ω_0 and $|2\epsilon|$ can be achieved, for example, in NMR by lowering the d.c. field. This limit implies that $\cos(\theta) \approx 0$, $\sin(\theta)$ approaches $+1$ or -1 corresponding to positive or negative ϵ respectively, and $\nu \approx |2\epsilon|$. The relaxation coefficients in the P representation then reduce to:

$$\begin{aligned}
&\Gamma_x \approx \tfrac{1}{4}\left[\Gamma_p^0(\omega - |2\epsilon|) + \Gamma_p^0(\omega + |2\epsilon|)\right] + \Gamma_d'^0(|2\epsilon|), \\
&\Gamma_y \approx \tfrac{1}{2}\,\Gamma_p^0(\omega) + \Gamma_d'^0(|2\epsilon|), \\
&\Gamma_z \approx \tfrac{1}{4}\left[\Gamma_p^0(\omega - |2\epsilon|) + 2\Gamma_p^0(\omega) + \Gamma_p^0(\omega + |2\epsilon|)\right], \\
&\Gamma_{xz} \approx 0, \\
&\Gamma_{zx} \approx \pm\tfrac{1}{4}\left[\Gamma_p^0(\omega - |2\epsilon|) - \Gamma_p^0(\omega + |2\epsilon|)\right], \\
&\gamma_z \approx \tfrac{1}{4}\left[\delta^0(\omega - |2\epsilon|) + 2\delta^0(\omega) + \delta^0(\omega + |2\epsilon|)\right], \\
&\gamma_x \approx \pm\left\{\tfrac{1}{4}\left[\delta^0(\omega + |2\epsilon|) - \delta^0(\omega - |2\epsilon|)\right] + \tfrac{1}{2}\,\alpha^0(|2\epsilon|)\right\}.
\end{aligned} \tag{5.7}$$

The $\pm$ sign corresponds to 2ϵ positive or negative respectively. For this case the coefficients associated with population relaxation differ from the ones in the SBE, and are explicitly field-dependent. Also, in this limit the coupling coefficient Γ_{xz} vanishes, whereas Γ_{zx} does not. Finally, note that if $|2\epsilon| \gg 1/\tau_c$ the pure dephasing mechanism is quenched and both $\alpha^0(|2\epsilon|)$ and $\Gamma_d'^0(|2\epsilon|)$ in Eq. (5.7) vanish.

VI. THE STEADY-STATE SOLUTION OF THE GENERALIZED BLOCH EQUATIONS AND A GENERALIZED THEORY FOR LINE-SHAPES

The dynamics induced by the GBE lead the TLS to a steady state (in the rotating frame). The steady-state power, directly related to the homogeneous line-shape, is examined

in this section. The steady-state expectation values of all the polarization components in the P representation are given explicitly in Appendix D.

The steady state is characterized by the TLS continuously absorbing energy from the field and rejecting it into the bath, in a manner that maintains energy balance. From a thermodynamical point of view, the work performed on the TLS by the field is completely dissipated and rejected as heat into the thermal bath, thereby increasing the entropy of the universe. Hence, the TLS must absorb energy from the field in steady state in order not to contradict the second law of thermodynamics. The absorption spectrum consists of the rate of energy absorbed by the TLS from the field, as a function of the field's frequency.

From Eqs. (3.3) and (4.33) the power, which is the rate of energy absorbed by the TLS from the field, becomes:

$$\mathscr{P}=\left\langle \frac{\partial \mathbf{W}}{\partial t}\right\rangle =2\epsilon\omega\langle\hat{\mathbf{P}}_{\mathbf{y}}\rangle=2\epsilon\omega\langle\hat{\mathbf{\Pi}}_{y}\rangle. \tag{6.1}$$

Note that $\langle\hat{\mathbf{P}}_{\mathbf{y}}\rangle = \langle\hat{\mathbf{\Pi}}_{y}\rangle$ since the transformation to the Π representation amounts to a rotation by θ around the rotating $\hat{y}$ axis. It therefore leaves the component of the polarization along the $\hat{y}$ axis invariant (cf. Fig. 3). The spectrum will be given by the steady-state power, $\mathscr{P}(\omega)$. In the plots that follow a line-shape function defined by:

$$LS(\omega)=\mathscr{P}(\omega)/\omega \tag{6.2}$$

is used.

Consider the power function obtained from the SBE, Eq. (4.35):

$$\mathscr{P}(\omega)=\frac{-\omega(2\epsilon)^2P_z^{eq}/T_2}{(\Delta\omega)^2+\left(\frac{1}{T_2}\right)^2+\frac{T_1}{T_2}(2\epsilon)^2}. \tag{6.3}$$

The corresponding standard line-shape is Lorentzian. The peak is at $\omega=\omega_0$, and the broadening has two contributions: $1/T_2^2$, from dephasing; and $(2\epsilon)^2\ T_1/T_2$, from power broadening.

A few important properties of the power function in Eq. (6.3) should be remarked upon.

(1) To be consistent with thermodynamics the power production of a TLS coupled to a positive temperature heat bath has to be a non-negative quantity. From Eq. (6.3) it can be learned that the power is non-negative only for positive ω. Therefore it fails to comply with this fundamental thermodynamical constraint for negative field frequencies. Recall that in the context of a circularly rotating driving field, as in this model, negative frequencies are well defined and physically distinguishable from positive ones. This inconsistency is not very important from the practical point of view since the standard theory only applies for weak fields, where the line-shape is very narrowly distributed around resonance.

(2) The power vanishes when the bath coupling operators $\mathbf{\Lambda}$ and $\mathbf{\Lambda}^\dagger$ vanish. In this limit $T_1\to\infty$, which from Eq. (6.3) leads to $\mathscr{P}(\omega)=0$. Once this coupling vanishes, there is no mechanism for energy transfer between the TLS and the bath, resulting in zero absorption in steady state (which is known as complete saturation). This should also hold for the GBE.

The power and line-shape functions obtained from the GBE are now analyzed. The line-shape function in terms of the P representation can be obtained by multiplying $\hat{P}_y^{ss}$ from Appendix D by 2ϵ. For the purposes of this section it is more convenient to work in the Π representation. Solving Eq. (4.29) for steady state and evaluating the power leads to the following expression:

$$\mathscr{P}(\omega)=\frac{-2\epsilon\omega\nu(\alpha\Gamma_p+\eta\delta)}{\Gamma_p\nu^2+\Gamma_p(\Gamma_d'+\frac{1}{2}\Gamma_p)^2-2\eta\xi(\lambda+\Gamma_d'+\frac{1}{2}\Gamma_p)-\lambda^2\Gamma_p} \tag{6.4}$$

[recall that $\nu=\sqrt{(\Delta\omega)^2+2(\epsilon)^2}$]. Equation (6.4) is a generalization of Eq. (6.3), and is applicable at arbitrary field intensities and frequencies. The exact line-shape predicted by Eq. (6.4) depends upon the specific physical realization of the bath. In principle the expression can be inverted to probe the bath properties. As an example, the line-shape in Eq. (6.4) is evaluated for the case of a Debye solid in the next section.

A few general properties of the generalized line-shape serve as crucial consistency tests and should be pointed out:

(1) The generalized line-shape converges to the standard Lorentzian line-shape [Eq. (6.3)] in weak fields (cf. Sec. V).

(2) The generalized power is non-negative for all frequencies, as is shown in Appendix E. This implies that, unlike the SBE, the generalized ones are consistent with the second law of thermodynamics for all field frequencies.

(3) The generalized line-shape vanishes when $\mathbf{\Lambda}$ and $\mathbf{\Lambda}^\dagger$ do, as is shown in Appendix E. Hence, the present model correctly describes the line-shape for arbitrary field intensities.

VII. AN ILLUSTRATIVE SPECIAL CASE: THE LINE-SHAPE OF A TLS IMPURITY EMBEDDED IN A DEBYE SOLID

The rate coefficients in the GBE and the corresponding line-shape depend upon the specific physical realization of the bath. In this section the line-shape of a TLS coupled to a Debye solid is analyzed.

For a bath consisting of the acoustic normal modes of a solid, the bath Hamiltonian is given by

$$\mathbf{H_b}=\sum_n\ \omega_n\mathbf{b_n^\dagger b_n}, \tag{7.1}$$

where ω_n, $\mathbf{b_n^\dagger}$ and $\mathbf{b_n}$ are the frequency, and creation and annihilation operators associated with the n-th mode. Consider $\mathbf{\Lambda}$ and $\mathbf{\Lambda}^\dagger$ to be linear, and $\mathbf{\Delta}$ quadratic, in the coordinates of the normal modes:[11,12]

$$\begin{aligned}\mathbf{\Lambda}&=\mathbf{\Lambda}^\dagger=\sum_n\ (g_n\mathbf{b_n}+g_n^*\mathbf{b_n^\dagger}),\\ \mathbf{\Delta}&=\sum_{i\neq j}\ (d_i\mathbf{b_i}+d_i^*\mathbf{b_i^\dagger})(d_j\mathbf{b_j}+d_j^*\mathbf{b_j^\dagger}).\end{aligned} \tag{7.2}$$

$\{g_n\}$ and $\{d_i\}$ are bath-TLS coupling coefficients. Note that $\langle \mathbf{\Lambda} \rangle_b = \langle \mathbf{\Lambda}^\dagger \rangle_b = \langle \mathbf{\Delta} \rangle_b = 0$.

The analysis starts by evaluating the bath parameters associated with the off-diagonal coupling, i.e. the coupling associated with $\mathbf{\Lambda}$ and $\mathbf{\Lambda}^\dagger$. The evaluation of $C_{\Lambda\Lambda^\dagger}(\tau)$ leads to

$$\begin{aligned} C_{\Lambda\Lambda^\dagger}(\tau) &= \sum_n |g_n|^2 \{ e^{-i\omega_n \tau}[1+n(\beta\omega_n)] \\ &\quad + e^{i\omega_n\tau} n(\beta\omega_n)\} \\ &\rightarrow \int_0^\infty d\omega \rho(\omega) |g(\omega)|^2 \{ e^{-i\omega\tau}[1+n(\beta\omega)] \\ &\quad + e^{i\omega\tau} n(\beta\omega)\}, \end{aligned} \tag{7.3}$$

where

$$n(x) = \frac{1}{e^x - 1}, \tag{7.4}$$

and $\rho(\omega)$ is the bath mode density. Continuous frequency, ω, and coupling coefficient, $g(\omega)$, replace their discrete analogues, ω_n and g_n. Note that ω and ρ in Eq. (7.3) *are not* the field frequency and the density operator from previous sections.

The evaluation of $\tilde{C}_{\Lambda\Lambda^\dagger}(x)$ yields

$$\tilde{C}_{\Lambda\Lambda^\dagger}(x) = \begin{cases} 2\pi\rho(x)|g(x)|^2[n(\beta x)+1] & \text{if } x>0 \\ 2\pi\rho(-x)|g(-x)|^2 n(-\beta x) & \text{if } x<0 \end{cases}. \tag{7.5}$$

Unlike in the field-free case, the sign of x need not be strictly positive or negative. This is why both lines in Eq. (7.5) are important, and a rotating wave approximation according to which $\mathbf{\Lambda} = \Sigma_n g_n \mathbf{b_n}$, $\mathbf{\Lambda}^\dagger = \Sigma_n g_n^* \mathbf{b_n^\dagger}$, was not introduced. In the latter approximation, $\tilde{C}_{\Lambda\Lambda^\dagger}(x)$ vanishes for negative x, and hence a physically unjustified bias is introduced into the rate coefficients.

Substituting Eq. (7.5) in Eqs. (4.31) yields

$$\Gamma_p^0(x) = 2\pi\rho(|x|)|g(|x|)|^2 \coth(\beta|x|/2), \tag{7.6}$$

$$\delta^0(x) = \begin{cases} \pi\rho(x)|g(x)|^2, & \text{if } x>0 \\ -\pi\rho(-x)|g(-x)|^2, & \text{if } x<0 \end{cases}. \tag{7.7}$$

In the Debye solid[11]

$$g(x) = \mu\sqrt{\frac{x}{2N}},$$

$$\rho(x) = \begin{cases} \frac{3N}{\omega_D^3} x^2, & \text{for } 0 \leqslant x \leqslant \omega_D \\ 0, & \text{otherwise} \end{cases}, \tag{7.8}$$

where ω_D is the Debye frequency, N is the total number of normal modes and μ is a coupling constant with units of square root of energy. Hence, in the Debye solid the relaxation coefficients Γ_p^0 and δ^0 are given by

$$\Gamma_p^0(x) = \begin{cases} 0, & \text{if } |x|>\omega_D \\ 3\pi\mu^2 \left|\frac{x}{\omega_D}\right|^3 \coth(\beta|x|/2), & \text{if } |x| \leqslant \omega_D \end{cases}, \tag{7.9}$$

$$\delta^0(x) = \begin{cases} 0, & \text{if } |x|>\omega_D \\ \frac{3}{2}\pi\mu^2 \left[\frac{x}{\omega_D}\right]^3, & \text{if } |x| \leqslant \omega_D \end{cases}. \tag{7.10}$$

The diagonal coupling correlation function associated with the bath operator $\mathbf{\Delta}$ is evaluated next. The evaluation of $C_{\Delta\Delta}(\tau)$ yields

$$\begin{aligned} C_{\Delta\Delta}(\tau) &= \sum_{k\neq l} 2|d_k|^2|d_l|^2 \{ e^{-i(\omega_k+\omega_l)\tau}[n(\beta\omega_k)+1][n(\beta\omega_l)+1] + e^{i(\omega_k+\omega_l)\tau} n(\beta\omega_k) n(\beta\omega_l) + 2e^{-i(\omega_k-\omega_l)\tau} \\ &\quad \times [n(\beta\omega_k)+1] n(\beta\omega_l)\} \\ &\rightarrow 2\int_0^\infty d\omega \rho(\omega)|d(\omega)|^2 \int_0^\infty d\omega' \rho(\omega')|d(\omega')|^2 \{ e^{-i(\omega+\omega')\tau}[n(\beta\omega)+1] \\ &\quad \times [n(\beta\omega')+1] + e^{i(\omega+\omega')\tau} n(\beta\omega) n(\beta\omega') + 2e^{-i(\omega-\omega')\tau}[n(\beta\omega)+1] n(\beta\omega')\}. \end{aligned} \tag{7.11}$$

On the last line of Eq. (7.11), continuous frequencies, ω and ω', and coupling coefficients, $d(\omega)$ and $d(\omega')$, replace their discrete analogues, ω_k, ω_l, d_k and d_l.

The evaluation of $\tilde{C}_{\Delta\Delta}(x)$ yields

$$\begin{aligned} \tilde{C}_{\Delta\Delta}(x) &= 8\pi \int_0^\infty d\omega \rho(\omega)\rho(\omega+x)|d(\omega)|^2|d(\omega+x)|^2 n(\beta\omega)[n(\beta(\omega+x))+1] + 4\pi \\ &\quad \times \int_0^\nu d\omega \rho(\omega)\rho(x-\omega)|d(\omega)|^2|d(x-\omega)|^2[n(\beta\omega)+1][n(\beta(x-\omega))+1]. \end{aligned} \tag{7.12}$$

In the Debye solid

$$d(x)=\sqrt{W}\,\tfrac{1}{2}\sqrt{x/2N}\ , \tag{7.13}$$

and $\rho(x)$ is given by Eq. (7.8). W is a dimensionless coupling coefficient. Substituting Eq. (7.8) and Eq. (7.13) in Eq. (7.12), which is substituted in turn into Eq. (4.31), yields $\Gamma_d'^0(x)$ and $\alpha^0(x)$ for the Debye solid.

The derivation of the GBE involves two approximations that may now be explicitly expressed in terms of the Debye model:

(1) The rate of decay of the bath fluctuations is approximately ω_D for $T>\omega_D$, or T for $T<\omega_D$ (recall that since $\hbar=k_B=1$, T and ω_D can be viewed as frequencies as well as energies). The bath correlation function decays very fast on the time scale of the relaxation of the TLS. Hence, this approximation is valid if

$$\Gamma_p^0,\Gamma_d'^0 \ll \begin{cases} \omega_D & \text{if } T>\omega_D \\ T & \text{if } T<\omega_D. \end{cases} \tag{7.14}$$

(2) The field frequency, ω, is fast on the time scale of the TLS relaxation. Hence

$$\Gamma_p^0,\Gamma_d'^0 \ll \omega. \tag{7.15}$$

The arguments of $\Gamma_p^0(\omega)$, $\Gamma_p^0(\omega\pm\nu)$, $\Gamma_d'(\nu)$, $\delta^0(\omega)$, $\delta^0(\omega\pm\nu)$, and $\alpha^0(\nu)$ depend upon the field amplitude and frequency. In the standard theory, they come with field-independent arguments, namely ω_0 and 0. The main implication is that $\Gamma_p^0(\omega)$, $\Gamma_p^0(\omega\pm\nu)$, $\Gamma_d'(\nu)$, $\delta^0(\omega)$, $\delta^0(\omega\pm\nu)$, and $\alpha^0(\nu)$ scan through *all* the bath frequencies as the field frequency is changed, and therefore provide a tool to probe the mode density of the bath. The most dominant feature in the mode density of the Debye solid is the cutoff at ω_D. The latter would lead to sharp cutoffs in the bath coefficients in the following cases:

(1) $\Gamma_p^0(\omega)$ and $\delta^0(\omega)$ experience a sharp cutoff at

$$\omega=\pm\omega_D. \tag{7.16}$$

(2) $\Gamma_p^0(\omega+\nu)$ and $\delta^0(\omega+\nu)$ experience a sharp cutoff when $\omega+\nu=\omega_D$. The latter equality can be reached only when $\omega_D>\omega_0$, at

$$\omega=\tfrac{1}{2}\left[\frac{\omega_0+\omega_D+(2\epsilon)^2}{\omega_D-\omega_0}\right], \tag{7.17}$$

which lies below ω_D.

(3) $\Gamma_p^0(\omega-\nu)$ and $\delta^0(\omega-\nu)$ experience a sharp cutoff when $\omega-\nu=\omega_D$. If $\omega_D<\omega_0$ the cutoff value is

$$\omega=\tfrac{1}{2}\left[\frac{\omega_0+\omega_D+(2\epsilon)^2}{\omega_D-\omega_0}\right], \tag{7.18}$$

which lies above ω_D. If $\omega_D>\omega_0$ the cutoff value is

$$\omega=\tfrac{1}{2}\left[\frac{\omega_0-\omega_D+(2\epsilon)^2}{\omega_D+\omega_0}\right]. \tag{7.19}$$

TABLE V. Parameters used in plotting the line-shapes for the Debye model. Also listed are the values of the field-free $1/T_1$ and $1/T_2'$.

case	T	μ	$1/T_1$	W	$1/T_2'$
(A)	0.1	0.001	1.8(−6)	0.0	0.0
(B)	0.1	0.001	1.8(−6)	0.2	1.3(−6)
(C)	0.1	1.0(−6)	1.8(−12)	0.2	1.3(−6)
(D)	1.0	0.001	2.5(−6)	0.0	0.0
(E)	1.0	0.001	2.5(−6)	0.001	2.3(−6)
(F)	1.0	1.0(−6)	2.5(−12)	0.001	2.3 (−6)
(G)	10.0	0.001	2.4(−5)	0.0	0.0
(H)	10.0	0.001	2.4(−5)	0.0003	2.6(−5)
(I)	10.0	1.0(−6)	2.4(−10)	0.0003	2.6(−5)

(4) $\Gamma_d'^0(\nu)$ and $\alpha^0(\nu)$ experience a sharp cutoff when $\nu=2\omega_D$. The cutoffs become

$$\omega=\omega_0\pm\sqrt{(2\epsilon)^2+(2\omega_D)^2}\ . \tag{7.20}$$

The line-shape was examined for various values of the parameters. Setting $\omega_0=1$ means that all energies, frequencies, temperatures and coupling constants are measured in units of ω_0. ω_D is also fixed in all the examples considered, and equals $2\omega_0$.

The temperature dependence of the line-shape is examined for low ($T=0.1$), medium ($T=1$) and high ($T=10$) values. Different relative values of the diagonal and nondiagonal coupling are considered. The values of the coupling parameters μ and W where chosen so that the approximations leading to the derivations are valid. Furthermore, the values of μ and W where chosen so that the field-free rate coefficients, $\Gamma_p^0(\omega_0)$ and $\Gamma_d'^0(0)$, are similar for different temperatures. The explicit values of μ and W that were used are presented in Table V.

The results for case (A) are presented in Fig. 4. Figure 4 demonstrates how the deviations from the standard line-shape increase as the field intensifies. At $\epsilon=0.025$ the deviations are quite small, and are manifested by a blue shift. At $\epsilon=0.1$, the blue shift increases and a distortion due to the cutoff is added to it. At $\epsilon=0.5$, the line-shape is completely distorted and bears no resemblance to the standard one. The loss of the typical bell shape is due to the fact that the blue shift approaches the cutoffs. Note that unlike the standard line-shape function [Eq. (6.3)], the line-shape obtained from the present model changes sign as negative frequencies are approached, so that the power remains non-negative (6.2), in accord with the second law of thermodynamics.

The line-shapes obtained for cases (B) and (C) are quite similar. They differ with respect to case (A) by the additional diagonal coupling. Therefore the results for the more extreme case (C), where the diagonal coupling is much stronger, are shown in Figs. 5 and 6. For small fields the picture is very similar to that in the standard theory, namely, a line-shape narrowly distributed around resonance. However, in Fig. 5, a significant wide band ''off-resonance'' absorption is seen at much higher frequencies. The latter increases and widens considerably as the field increases, and finally merges with the blue-shifted resonance peak (cf. Fig. 6). As the saturation further increases, the line-shape is completely dis-

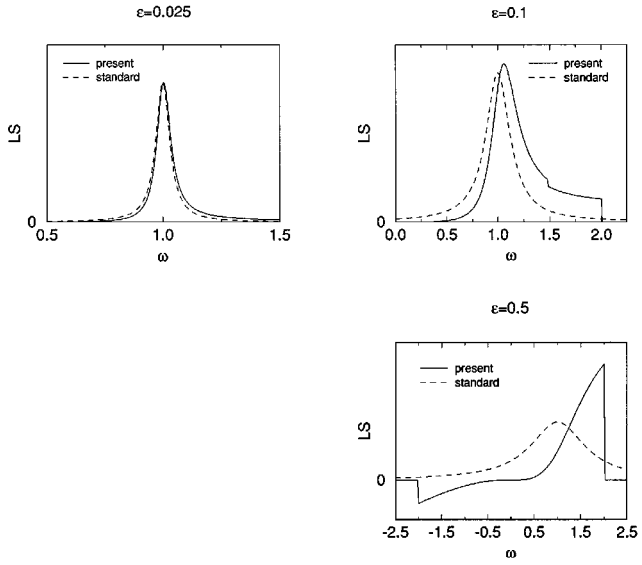

FIG. 4. Comparison of the line-shape obtained from the SBE and the GBE for a TLS impurity embedded in a Debye solid. The units are such that energies and frequencies are measured in units of ω_0 (i.e. $\omega_0=1$). The parameters used to evaluate the line-shapes are: $\omega_D=2$, $\mu=0.001$, $W=0$, $T=0.1$. Note that only off-diagonal coupling is accounted for in this case ($W=0$). The three plots correspond to different field intensities: $\epsilon=0.025$, $\epsilon=0.1$, $\epsilon=0.5$. The deviations between the SBE and GBE results are more pronounced for higher field intensities. The effects of the Debye cutoff on the line-shape is observed for $\epsilon=0.1$ and $\epsilon=0.5$. The inconsistency of the SBE for negative field frequencies is demonstrated for $\epsilon=0.5$.

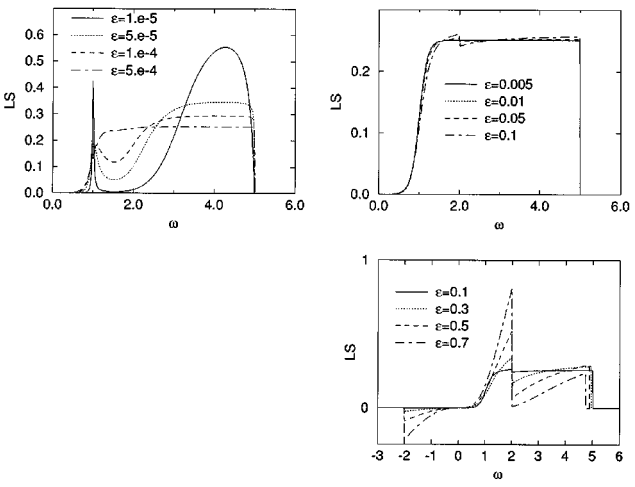

FIG. 6. Line-shapes obtained from the GBE for the same parameters as in Fig. 5, but for higher field intensities. The area under each line-shape is normalized to 1. The units are such that energies and frequencies are measured in units of ω_0 (i.e. $\omega_0=1$).

torted, and the off-diagonal coupling become dominant, leading to line-shapes similar to those obtained in case (A) for very high fields.

The line-shapes obtained for case (D) are similar to these obtained for case (A). Cases (E) and (F) provide new features due to the additional diagonal coupling; examining the more extreme case (F), the results are shown in Fig. 7. For lower fields the picture resembles that obtained for case (A).

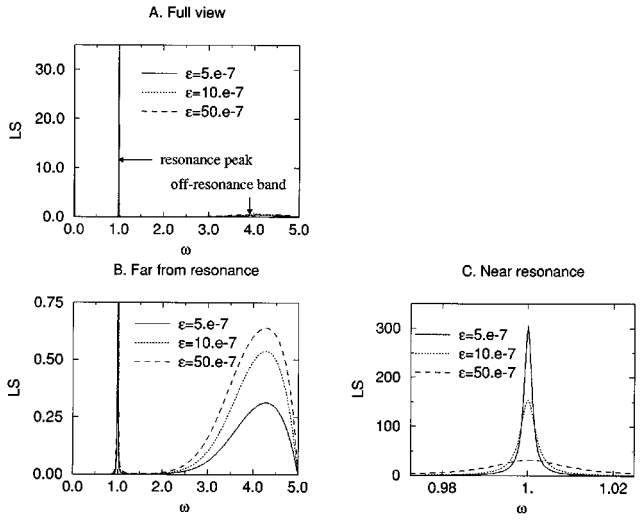

FIG. 5. Line-shapes obtained from the GBE for relatively low field intensities ($\epsilon \leqslant 5\times10^{-6}$). The area under each line-shape is normalized to 1. The units are such that energies and frequencies are measured in units of ω_0 (i.e. $\omega_0=1$). The parameters used to evaluate the line-shapes are $\omega_D=2$, $\mu=1\times10^{-6}$, $W=0.2$, $T=0.1$. The line-shapes are shown on the full frequency scale in graph A (note that the resonance peak was truncated at about one-tenth of its actual height). The wide off-resonance absorption band around $\omega=4$ is magnified on graph B. The full resonance peak is shown on a narrow frequency scale on graph C.

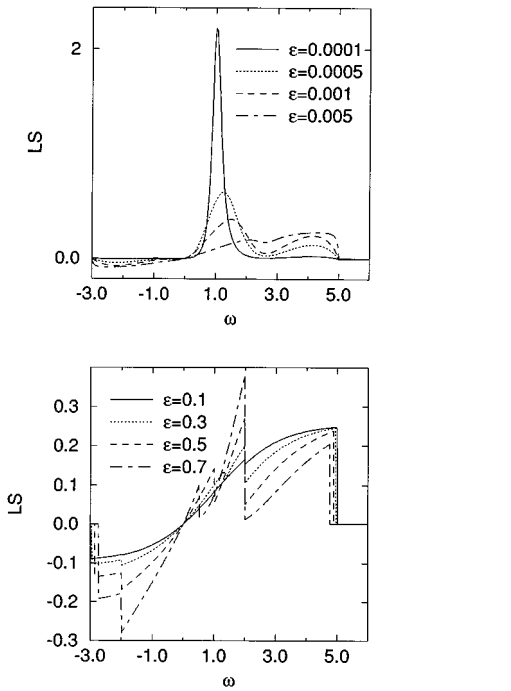

FIG. 7. Line-shapes obtained from the GBE for various field intensities. The area under each line-shape is normalized to 1. The units are such that energies and frequencies are measured in units of ω_0 (i.e. $\omega_0=1$). The parameters used to evaluate the line-shapes are: $\omega_D=2$, $\mu=1\times10^{-6}$, $W=0.001$, $T=1.0$.

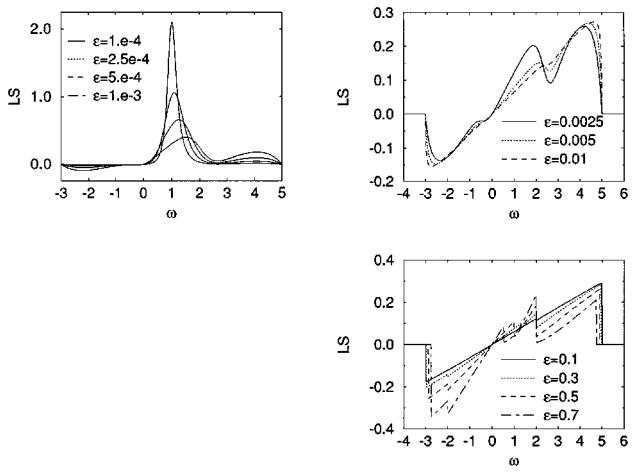

FIG. 8. Line-shapes obtained from the GBE for various field intensities. The area under each line-shape is normalized to 1. The units are such that energies and frequencies are measured in units of ω_0 (i.e. $\omega_0=1$). The parameters used to evaluate the line-shapes are: $\omega_D=2$, $\mu=1\times10^{-6}$, $W=0.0003$, $T=10.0$.

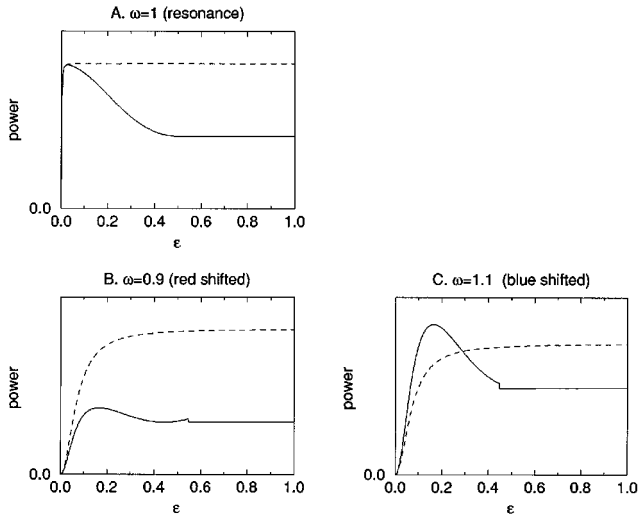

FIG. 9. Comparison of saturation curves (power vs. field intensity) obtained from the SBE and the GBE. The dashed curves correspond to the SBE and the continuous curves to the GBE. The units are such that energies and frequencies are measured in units of ω_0 (i.e. $\omega_0=1$). Graph A corresponds to resonance, graph B corresponds to a frequency red-shifted with respect to resonance, and graph C corresponds to a frequency blue-shifted with respect to resonance. The other parameters for this plot are: $\omega_D=2$, $T=1.0$, $\mu=0.05$, and $W=0$.

For higher fields, the line-shape acquires a highly toothed character due to the various cutoffs.

The line-shapes obtained for case (G) are similar to these obtained for cases (A) and (D). Cases (H) and (I) provide interesting features that are, as before, due to the diagonal coupling. As before, the more extreme case (I) is shown in Fig. 8. The pattern resembles that in Fig. 7. The ''wavy'' nature of the line-shape preceding the high field ''toothed'' line-shape is interesting to note.

In conclusion, the line-shapes obtained close to saturation show great diversity and complexity, and contain nonlocal information on the density of bath modes and the nature of the coupling with the bath. It should be noted however that extracting this information might not be easy, and certainly requires a detailed model for the TLS-bath interaction.

The saturation of the power is presented by plotting the power vs. the Rabi frequency at a given frequency. The results of the GBE are presented and compared to those obtained from the SBE in Figs. 9–11. Generally, the behaviour at saturation differs significantly from that predicted by the standard theory, which is not consistent at saturation. The saturation behaviour is a direct manifestation of the explicit dependence of the bath terms upon the parameters of the field. In saturation, the dominant term in the denominator of the power function is $\Gamma_p(2\epsilon)^2$. $(2\epsilon)^2$ factors out with the corresponding term in the numerator, so that the power is proportional to $(\alpha\Gamma_p+\eta\delta)/\Gamma_p$. The dependence of the latter upon the field parameters yields the different saturation behaviours shown in Figs. 9–11.

VIII. RELATION TO OTHER STUDIES AND CONCLUDING REMARKS

The first attempt to generalize the Bloch equations to the domain of intense driving fields was carried out in NMR. The motivation was provided by Redfield's demonstration of the failure of the SBE to account for the experimental NMR signals in solids, under the conditions of saturation.[18] From the attempts to construct a theory for nuclear spin relaxation under the conditions of saturation, the pioneering studies of Bloch[19] and Tomita[20] are most relevant to the present study. In both cases, the derivation of the GBE follows a similar procedure, where the basic idea is to transform to the rotating frame tilted by the angle θ with respect to the original z axis, and carry out the derivation of the master equation in this representation. Naturally, the advances made in the theory of open quantum systems since the papers of Bloch and Tomita were published should be

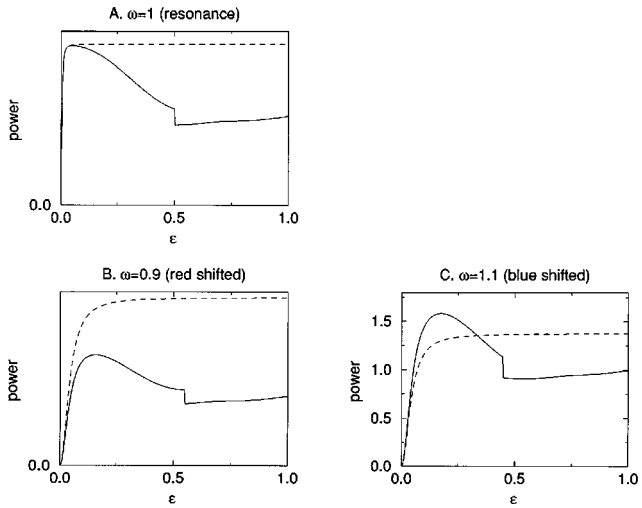

FIG. 10. Same as Fig. 9 but with parameters $\omega_D=2$, $T=1.0$, $\mu=0.05$, and $W=0.05$.

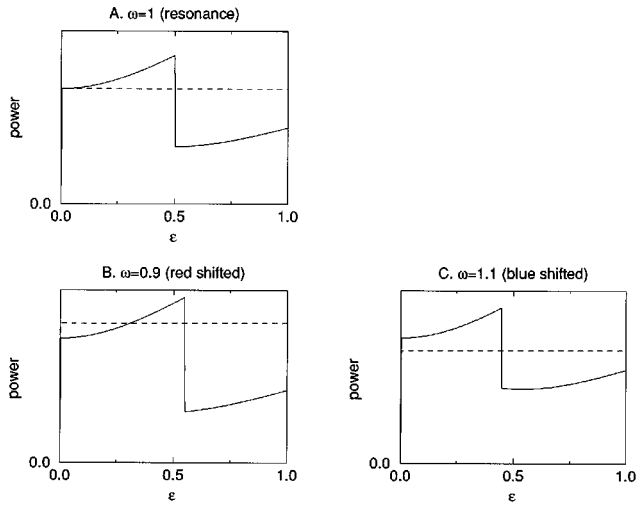

FIG. 11. Same as Fig. 9 but with parameters $\omega_D=2$, $T=1.0$, $\mu=1\times10^{-6}$, and $W=0.05$.

incorporated. As a result, the present treatment is more satisfactory from the mathematical point of view, but the general results are similar.

The more important difference between the work of Bloch and Tomita and the present study lies in the different points of view. The work of Bloch and Tomita was directed towards applications in NMR. The present study views a general TLS of arbitrary origin, and examines what can be *generally* said about its relaxation in strong fields without adopting specific relaxation mechanisms or employing simplifying approximations. For example, Tomita employs the high-temperature limit and exponentially decaying bath correlation functions at a very early stage of the derivation, making it difficult to see which of the results rely on these assumptions.

The more modern treatments of the problem of relaxation in strong fields were motivated by experimental evidence for the failure of the SBE to explain the free-induction decay following saturation of an electronic transition of $\mathbf{Pr^{3+}}$ impurity embedded in $\mathbf{LaF_3}$.[23] The treatments in the spirit of the present work are mainly those in Refs. 29–32. These treatments are even more specific then the ones in NMR, and differ from the present study in the following respects: (1) they consider only pure-dephasing-type diagonal interactions with the bath, and treat population relaxation phenomenologically; (2) they consider a semiclassical time-dependent Hamiltonian with stochastic fluctuations (except for Ref. 30). We show how the generalized optical Bloch equations obtained by these authors follow naturally from our more general fully quantum-mechanical results in the appropriate limits.

A different approach for the proper description of relaxation in systems subject to time-dependent fields was utilized in previous studies.[43–45] The latter is based on the hypothesis that the relaxation dynamics is constantly guiding the system towards an equilibrium state corresponding to the instantaneous Hamiltonian. The field-dependent relaxation equation thus obtained should hold in the case of a sufficiently slowly varying field. In such a case, the field may be taken as approximately constant throughout the time interval for which the solution of the Liouville equation is repeatedly approximated by a second-order perturbation expansion. The analysis of the present work assumes that terms rotating with the field average out throughout the very same time interval. This assumption is therefore in conflict with that required for the equations of Refs. 43–45 to hold, since the field can either rotate fast or remain constant at this time interval, but certainly not both. Hence, the GBE presented here are adequate in the ''fast field'' regime, whereas the approach of Refs. 43–45 is required for the derivation of analogous equations in the ''slow field'' regime.

To summarize, the main results of the present study are: (1) a general, unified, comprehensive, and fully quantum-mechanical derivation of the generalized Bloch equations; (2) a careful analysis showing under which weak-field circumstances the standard Bloch equations are valid; (3) the demonstration that the generalized optical Bloch equations follow naturally in certain limits from the generalized Bloch equations; (4) the introduction of the thermodynamic point of view as a tool for examining the generalized Bloch equations; and (5) the demonstration that line-shapes near saturation can provide information about bath spectral densities. As the use of intense fields becomes more routine, the necessity of using the generalized Bloch equations will become increasingly apparent, as will the richness they contain.

ACKNOWLEDGMENTS

We thank Peter Salamon and Steve Berry for stimulating discussions. This research was supported by the Binational United States - Israel Science Foundation and the Israel Science Foundation. The Fritz Haber Research Centers is supported by the Minerva Gesellschaft für die Forschung, GmbH München, FRG. J.L.S. acknowledges support from the Guggenheim and Humboldt Foundations and from (US) NSF Grant No. CHE92-19474.

APPENDIX A: THE EVALUATION OF THE BATH FACTORS

In this appendix the evaluation of the first bath factor in Eq. (4.24) is described. The other bath factors are evaluated in a similar manner.

Consider the first bath factor:

$$\int_0^t dt_1 \mathrm{Tr_b}(\tilde{\mathcal{G}}(t)\tilde{\mathcal{G}}(t_1)\rho_b). \tag{A1}$$

The bath operators $\tilde{\mathcal{G}}(t)$ and $\tilde{\mathcal{G}}(t_1)$ are given in terms of the original bath operators in Eqs. (4.17)-(4.18). Thus,

$$\begin{aligned}\tilde{\mathscr{G}}(t)\tilde{\mathscr{G}}(t_1)&=e^{i\nu t}\{\cos^2(\theta/2)e^{i\omega t}\mathbf{\Lambda}(t)-\sin^2(\theta/2)e^{-i\omega t}\mathbf{\Lambda}^\dagger(t)-\tfrac{1}{2}\sin(\theta)\mathbf{\Delta}(t)\}\\&\times e^{i\nu t_1}\{\cos^2(\theta/2)e^{i\omega t_1}\mathbf{\Lambda}(t_1)-\sin^2(\theta/2)e^{-i\omega t_1}\mathbf{\Lambda}^\dagger(t_1)-\tfrac{1}{2}\sin(\theta)\mathbf{\Delta}(t_1)\}\\&=e^{2i\nu t}e^{-i\nu(t-t_1)}\{\cos^4(\theta/2)e^{2i\omega t}e^{-i\omega(t-t_1)}\mathbf{\Lambda}(t)\mathbf{\Lambda}(t_1)-\sin^2(\theta/2)\cos^2(\theta/2)e^{i\omega(t-t_1)}\mathbf{\Lambda}(t)\mathbf{\Lambda}^\dagger(t_1)\\&-\tfrac{1}{2}\sin(\theta)\cos^2(\theta/2)e^{i\omega t}\mathbf{\Lambda}(t)\mathbf{\Delta}(t_1)-\sin^2(\theta/2)\cos^2(\theta/2)e^{-i\omega(t-t_1)}\mathbf{\Lambda}^\dagger(t)\mathbf{\Lambda}(t_1)+\sin^4(\theta/2)e^{-2i\omega t}e^{i\omega(t-t_1)}\\&\times\mathbf{\Lambda}^\dagger(t)\mathbf{\Lambda}^\dagger(t_1)+\tfrac{1}{2}\sin(\theta)\sin^2(\theta/2)e^{-i\omega t}\mathbf{\Lambda}^\dagger(t)\mathbf{\Delta}(t_1)-\tfrac{1}{2}\sin(\theta)\cos^2(\theta/2)e^{i\omega t}e^{-i\omega(t-t_1)}\mathbf{\Delta}(t)\mathbf{\Lambda}(t_1)\\&+\tfrac{1}{2}\sin(\theta)\sin^2(\theta/2)e^{-i\omega t}e^{i\omega(t-t_1)}\mathbf{\Delta}(t)\mathbf{\Lambda}^\dagger(t_1)+\tfrac{1}{4}\sin^2(\theta)\mathbf{\Delta}(t)\mathbf{\Delta}(t_1)\}.\end{aligned}\tag{A2}$$

For the future we note that the common factor $e^{2i\nu t}$ will cancel out when transforming back from the interaction picture since

$$e^{-i\hat{\mathbf{H}}_s t}[\mathbf{\Pi}_+,\mathbf{\Pi}_+\hat{\sigma}]e^{i\hat{\mathbf{H}}_s t}=e^{-2i\nu t}[\mathbf{\Pi}_+,\mathbf{\Pi}_+\hat{\sigma}]\ .\tag{A3}$$

Taking the product of Eq. (A2) with ρ_b, performing the trace over the bath, and integrating one obtains

$$\begin{aligned}&\int_0^t dt_1\{\mathrm{Tr}_b(\tilde{\mathscr{G}}(t)\tilde{\mathscr{G}}(t_1)\rho_b)\}\\&=e^{2i\nu t}\Big\{\cos^4(\theta/2)e^{2i\omega t}\int_0^t d\tau e^{-i(\omega+\nu)\tau}C_{\Lambda\Lambda}(\tau)-\tfrac{1}{4}\sin^2(\theta)\int_0^t d\tau e^{i(\omega-\nu)\tau}C_{\Lambda\Lambda^\dagger}(\tau)-\tfrac{1}{2}\sin(\theta)\cos^2(\theta/2)e^{i\omega t}\\&\times\int_0^t d\tau e^{-i\nu\tau}C_{\Lambda\Delta}(\tau)-\tfrac{1}{4}\sin^2(\theta)\int_0^t d\tau e^{-i(\omega+\nu)\tau}C_{\Lambda^\dagger\Lambda}(\tau)+\sin^4(\theta/2)e^{-2i\omega t}\int_0^t d\tau e^{i(\omega-\nu)\tau}C_{\Lambda^\dagger\Lambda^\dagger}(\tau)+\tfrac{1}{2}\sin(\theta)\sin^2(\theta/2)\\&\times e^{-i\omega t}\int_0^t d\tau e^{-i\nu\tau}C_{\Lambda^\dagger\Delta}(\tau)-\tfrac{1}{2}\sin(\theta)\cos^2(\theta/2)e^{i\omega t}\int_0^t d\tau e^{-i(\omega+\nu)\tau}C_{\Delta\Lambda}(\tau)+\tfrac{1}{2}\sin(\theta)\sin^2(\theta/2)e^{-i\omega t}\\&\times\int_0^t d\tau e^{i(\omega-\nu)\tau}C_{\Delta\Lambda^\dagger}(\tau)+\tfrac{1}{4}\sin^2(\theta)\int_0^t d\tau e^{-i\nu\tau}C_{\Delta\Delta}(\tau)\Big\}.\end{aligned}\tag{A4}$$

$C_{AB}(\tau)$ with $A,B=\Lambda,\Lambda^\dagger,\Delta$ are bath correlation functions, defined in Eq. (4.25). Note that the integration variable was changed from t_1 into $\tau=t-t_1$.

Two approximations are now introduced that considerably simplify Eq. (A4).

(a) t in the upper limit of the integrals is substituted by ∞. This is a valid approximation if the decay of the bath correlations is very fast on the time scale of the TLS relaxation.

(b) Terms rotating like $e^{\pm i\omega t}$ or $e^{\pm 2i\omega t}$ are neglected. This is a valid approximation if the frequency of the field is very fast on the time scale of the TLS relaxation. Note that this approximation is used in the rotating frame. Introducing the same approximation in the stationary frame would mean averaging out the term corresponding to the interaction of the TLS with the driving field.

Following the second approximation, six of the nine terms in Eq. (A4) are eliminated. The remaining terms are those associated with $C_{\Lambda\Lambda^\dagger}(\tau)$, $C_{\Lambda^\dagger\Lambda}(\tau)$ and $C_{\Delta\Delta}(\tau)$. The other bath factors also turn out to be associated with only those correlation functions. Following the first approximation the remaining integrals may be evaluated using the relation:

$$\int_0^\infty d\tau e^{i\omega_0\tau}C_{AB}(\tau)=\frac{1}{2}\,\tilde{C}_{AB}(\omega_0)+\frac{1}{2\pi i}\mathscr{P}\int_{-\infty}^{\infty}d\omega\,\frac{\tilde{C}_{AB}(\omega)}{\omega-\omega_0},\tag{A5}$$

where $\tilde{C}_{AB}(x)$ is the Fourier transform of $C_{AB}(\tau)$:

$$\tilde{C}_{AB}(x)=\int_{-\infty}^{\infty}d\tau e^{ix\tau}C_{AB}(\tau),\tag{A6}$$

and $\mathscr{P}$ denotes the Cauchy value of the integral. When **A** and **B** are Hermitian conjugates, $\tilde{C}_{AB}(\omega)$ is both real and positive. This occurs for correlation functions of Λ with $\Lambda^\dagger$ and Δ with itself. However these are the only correlation functions remaining after the second approximation. Thus, Eq. (1.5) provides a convenient separation of the bath factor into real and imaginary parts. The imaginary part contributes to the oscillatory Hamiltonian dynamics and will eventually lead to small modifications of the detuning and the Rabi frequency[20] and are therefore neglected henceforth. The bath factor then turns into (except for a trivial oscillatory factor) a real positive time-independent relaxation rate coefficient that introduces a non-oscillatory, dissipative, contribution into the overall dynamics.

In conclusion, the first bath factor is approximated by

$$\int_0^t dt_1\{\mathrm{Tr}_b(\tilde{\mathscr{G}}(t)\tilde{\mathscr{G}}(t_1)\rho_b)\}\approx e^{2i\nu t}\gamma_1,$$

where

$$\begin{aligned}\gamma_1=\tfrac{1}{8}\sin^2(\theta)\{&-\tilde{C}_{\Lambda\Lambda^\dagger}(\omega-\nu)-e^{-\beta(\omega+\nu)}\tilde{C}_{\Lambda\Lambda^\dagger}(\omega+\nu)\\&+e^{-\beta\nu}\tilde{C}_{\Delta\Delta}(\nu)\}\end{aligned}\tag{A7}$$

is real and positive. Note that to obtain Eq. (A.7) the identity:

$$\tilde{C}_{AB}(-x)=e^{-\beta x}\tilde{C}_{BA}(x) \tag{A8}$$

is used.

APPENDIX B: THE RATE COEFFICIENTS $\gamma_1 \ldots \gamma_9$

The rate coefficients $\gamma_1 \ldots \gamma_9$ are real time-independent, yet field-dependent. They are given in terms of the Fourier transforms of the nonvanishing bath correlation functions:

$$\gamma_1=\tfrac{1}{8}\sin^2(\theta)\{-\tilde{C}_{\Lambda\Lambda^\dagger}(\omega-\nu)-e^{-\beta(\omega+\nu)}\tilde{C}_{\Lambda\Lambda^\dagger}(\omega+\nu)+e^{-\beta\nu}\tilde{C}_{\Delta\Delta}(\nu)\},$$

$$\gamma_2=\tfrac{1}{2}\{\cos^4(\theta/2)\tilde{C}_{\Lambda\Lambda^\dagger}(\omega+\nu)+\sin^4(\theta/2)e^{-\beta(\omega-\nu)}\times\tilde{C}_{\Lambda\Lambda^\dagger}(\omega-\nu)+\tfrac{1}{4}\sin^2(\theta)\tilde{C}_{\Delta\Delta}(\nu)\},$$

$$\gamma_3=\tfrac{1}{2}\sin(\theta)\{\cos^2(\theta/2)\tilde{C}_{\Lambda\Lambda^\dagger}(\omega)-\sin^2(\theta/2)e^{-\beta\omega}\tilde{C}_{\Lambda\Lambda^\dagger}(\omega)-\tfrac{1}{2}\cos(\theta)\tilde{C}_{\Delta\Delta}(0)\},$$

$$\gamma_4=\tfrac{1}{2}\left\{\sin^4(\theta/2)\tilde{C}_{\Lambda\Lambda^\dagger}(\omega-\nu)+\cos^4(\theta/2)e^{-\beta(\omega+\nu)}\times\tilde{C}_{\Lambda\Lambda^\dagger}(\omega+\nu)+\frac{1}{4}\sin^2(\theta)e^{-\beta\nu}\tilde{C}_{\Delta\Delta}(\nu)\right\},$$

$$\gamma_5=\tfrac{1}{8}\sin^2(\theta)\{-\tilde{C}_{\Lambda\Lambda^\dagger}(\omega+\nu)-e^{-\beta(\omega-\nu)}\tilde{C}_{\Lambda\Lambda^\dagger}(\omega-\nu)+\tilde{C}_{\Delta\Delta}(\nu)\},$$

$$\gamma_6=\tfrac{1}{2}\sin(\theta)\{-\sin^2(\theta/2)\tilde{C}_{\Lambda\Lambda^\dagger}(\omega)+\cos^2(\theta/2)e^{-\beta\omega}\tilde{C}_{\Lambda\Lambda^\dagger}(\omega)-\tfrac{1}{2}\cos(\theta)\tilde{C}_{\Delta\Delta}(0)\},$$

$$\gamma_7=\tfrac{1}{2}\sin(\theta)\{-\sin^2(\theta/2)\tilde{C}_{\Lambda\Lambda^\dagger}(\omega-\nu)+\cos^2(\theta/2)\times e^{-\beta(\omega+\nu)}\tilde{C}_{\Lambda\Lambda^\dagger}(\omega+\nu)-\tfrac{1}{2}\cos(\theta)e^{-\beta\nu}\tilde{C}_{\Delta\Delta}(\nu)\},$$

$$\gamma_8=\tfrac{1}{2}\sin(\theta)\{\cos^2(\theta/2)\tilde{C}_{\Lambda\Lambda^\dagger}(\omega+\nu)-\sin^2(\theta/2)\times e^{-\beta(\omega-\nu)}\tilde{C}_{\Lambda\Lambda^\dagger}(\omega-\nu)-\tfrac{1}{2}\cos(\theta)\tilde{C}_{\Delta\Delta}(\nu)\},$$

$$\gamma_9=\tfrac{1}{2}\{\sin^2(\theta)\tilde{C}_{\Lambda\Lambda^\dagger}(\omega)+\sin^2(\theta)e^{-\beta\omega}\tilde{C}_{\Lambda\Lambda^\dagger}(\omega)+\cos^2(\theta)\tilde{C}_{\Delta\Delta}(0)\}. \tag{B1}$$

Note that $\tilde{C}_{\Lambda\Lambda^\dagger}$ comes with the arguments ω and $\omega\pm\nu$, and $\tilde{C}_{\Delta\Delta}$ comes with the arguments ν and 0.

As the field is turned off ($\theta=0,\pi$), the only surviving terms are γ_2, γ_4 and γ_9. $\gamma_2+\gamma_4$ turns into $\frac{1}{2}\tilde{C}_{\Lambda\Lambda^\dagger}(\omega_0)\times(1+e^{-\beta\omega_0})$, and γ_9 turns into $\frac{1}{2}\tilde{C}_{\Delta\Delta}(0)$. These results are expected in the case of field-free relaxation.

APPENDIX C: TRANSFORMATION OF THE GENERALIZED MASTER EQUATION TO THE HEISENBERG PICTURE

In this Appendix the generalized master equation in Eq. (4.24) is transformed to the Heisenberg picture.

Starting with Liouville equation in the Schrödinger picture [Eq. (2.1)] it was transformed first to the rotating frame [Eq. (4.2)], and afterwards to the interaction picture [Eq. (4.15)]. Thus, Eq. (4.24) is given in terms of the ''Schrödinger-rotating-interaction picture.'' To transform to the Heisenberg picture, first a transformation back to the Schrödinger picture is carried out.

The transformation back from the interaction picture was described during the evaluation of the bath factors (cf. Appendix A). The transformation back from the rotating frame then amounts to replacing $\mathbf{P}_+$ by $e^{-i\omega t}\mathbf{P}_+$ and $\mathbf{P}_-$ by $e^{i\omega t}\mathbf{P}_-$.

The transformation from the Schrödinger picture to the Heisenberg picture is carried out by the following identity:

$$\frac{d}{dt}\langle\mathbf{X}\rangle\equiv\mathrm{Tr}(\mathscr{L}(\sigma)\cdot\mathbf{X})\equiv\mathrm{Tr}(\sigma\cdot\mathscr{L}^*(\mathbf{X})), \tag{C1}$$

where $\mathscr{L}$ is the generator of motion in the Schrödinger picture and $\mathscr{L}^*$ is the generator of motion in the Heisenberg picture. Note that the Tr in Eq. (C1) refer to a trace over the Hilbert space of the TLS. The identity comes about since the last two terms of Eq. (C1) equal the time derivative of the expectation value of the operator **X,** as given in the two pictures.

$\mathscr{L}$ is known from the master equation in the Schrödinger picture. It consists of Hamiltonian and dissipative parts:

$$\dot{\sigma}=\mathscr{L}(\sigma)=\mathscr{L}_H(\sigma)+\mathscr{L}_D(\sigma)\ , \tag{C2}$$

where

$$\mathscr{L}_H(\sigma)=-i[\mathbf{H_s^0}+\mathbf{W}(t),\sigma],$$

$$\mathscr{L}_D(\sigma)=\{-\gamma_1[\hat{\mathbf{\Pi}}_+,\hat{\mathbf{\Pi}}_+\sigma]-\gamma_2[\hat{\mathbf{\Pi}}_+,\hat{\mathbf{\Pi}}_-\sigma]-\gamma_3[\hat{\mathbf{\Pi}}_+,\hat{\mathbf{\Pi}}_z\sigma]-\cdots-\gamma_9[\hat{\mathbf{\Pi}}_z,\hat{\mathbf{\Pi}}_z\sigma]\}+\mathrm{h.c.} \tag{C3}$$

$\hat{\mathbf{\Pi}}_+$, $\hat{\mathbf{\Pi}}_-$, and $\hat{\mathbf{\Pi}}_z$ are the $\hat{\mathbf{\Pi}}$ operators in the rotating frame as defined in Eq. (4.27). It is well known that the Hamiltonian part transforms to the Heisenberg picture such that:

$$\mathscr{L}^*_{\mathscr{H}}(\mathbf{X})=i[\mathbf{H_s^0}+\mathbf{W}(t),\mathbf{X}]\ . \tag{C4}$$

The dissipative part is a sum of terms, each associated with a commutator of the following structure: $[\mathbf{A},\mathbf{B}\sigma]$ and its Hermitian conjugate. Each commutator is transformed by using Eq. (C1) and elementary properties of the trace:

$$\begin{aligned}\mathrm{Tr}\{[\mathbf{A},\mathbf{B}\sigma]\cdot\mathbf{X}\}&=\mathrm{Tr}\{\mathbf{AB}\sigma\mathbf{X}\}-\mathrm{Tr}\{\mathbf{B}\sigma\mathbf{AX}\}\\&=\mathrm{Tr}\{\sigma\mathbf{XAB}\}-\mathrm{Tr}\{\sigma\mathbf{AXB}\}\\&=\mathrm{Tr}\{\sigma\cdot[\mathbf{X},\mathbf{A}]\mathbf{B}\}.\end{aligned} \tag{C5}$$

The Hermitian conjugate is similarly obtained by

$$\mathrm{Tr}\{[\mathbf{A},\mathbf{B}\sigma]^{\dagger}\cdot\mathbf{X}\}=\mathrm{Tr}\{\sigma\cdot\mathbf{B}^{\dagger}[\mathbf{A}^{\dagger},\mathbf{X}]\}. \tag{C6}$$

Thus,

$$\mathscr{L}_D^*(\mathbf{X})=-\gamma_1([\mathbf{X},\hat{\mathbf{\Pi}}_+]\hat{\mathbf{\Pi}}_+ +\hat{\mathbf{\Pi}}_-[\hat{\mathbf{\Pi}}_-,\mathbf{X}])\cdots -\gamma_9([\mathbf{X},\hat{\mathbf{\Pi}}_z]\hat{\mathbf{\Pi}}_z+\hat{\mathbf{\Pi}}_z[\hat{\mathbf{\Pi}}_z,\mathbf{X}]). \tag{C7}$$

APPENDIX D: THE STEADY-STATE SOLUTION OF THE GENERALIZED BLOCH EQUATIONS IN THE *P* REPRESENTATION

The steady-state solution of Eq. (4.34) is obtained by equating the right-hand side to zero and solving for the steady-state expectation values of $\hat{\mathbf{P}}_\mathbf{x}$, $\hat{\mathbf{P}}_\mathbf{y}$ and $\hat{\mathbf{P}}_\mathbf{z}$, denoted by $\hat{P}_x^{ss}$, $\hat{P}_y^{ss}$ and $\hat{P}_z^{ss}$:

$$\hat{P}_x^{ss}=\frac{-2\epsilon\Delta\omega\,\frac{\gamma_z}{\Gamma_z}-\left[(2\epsilon)^2\frac{\gamma_x}{\Gamma_z}+\Gamma_y\gamma_x+\frac{\gamma_z\Gamma_{xz}}{\Gamma_z}\right]}{(\Delta\omega)^2+\frac{\Gamma_x}{\Gamma_z}(2\epsilon)^2+\Gamma_x\Gamma_y-\left[2\epsilon\Delta\omega\,\frac{\Gamma_{xz}+\Gamma_{zx}}{\Gamma_z}+\frac{\Gamma_y}{\Gamma_z}\,\Gamma_{xz}\Gamma_{zx}\right]},$$

$$\hat{P}_y^{ss}=\frac{2\epsilon\Gamma_x\frac{\gamma_z}{\Gamma_z}+\left[2\epsilon\Gamma_{zx}\frac{\gamma_x}{\Gamma_z}-\Delta\omega\left(\gamma_x+\Gamma_{xz}\frac{\gamma_z}{\Gamma_z}\right)\right]}{(\Delta\omega)^2+\frac{\Gamma_x}{\Gamma_z}(2\epsilon)^2+\Gamma_x\Gamma_y-\left[2\epsilon\Delta\omega\,\frac{\Gamma_{xz}+\Gamma_{zx}}{\Gamma_z}+\frac{\Gamma_y}{\Gamma_z}\,\Gamma_{xz}\Gamma_{zx}\right]},$$

$$\hat{P}_z^{ss}=\frac{-\frac{\gamma_z}{\Gamma_z}(\Gamma_x\Gamma_y+(\Delta\omega)^2)-\left[\frac{\gamma_x}{\Gamma_z}(2\epsilon\Delta\omega+\Gamma_y\Gamma_{zx})\right]}{(\Delta\omega)^2+\frac{\Gamma_x}{\Gamma_z}(2\epsilon)^2+\Gamma_x\Gamma_y-\left[2\epsilon\Delta\omega\,\frac{\Gamma_{xz}+\Gamma_{zx}}{\Gamma_z}+\frac{\Gamma_y}{\Gamma_z}\,\Gamma_{xz}\Gamma_{zx}\right]}. \tag{D1}$$

The terms in square brackets vanish when the SBE are valid, since $\gamma_x,\Gamma_{xz},\Gamma_{zx}\approx 0$ in such a case. The rest of the terms then reduce to the typical ''Lorentzian behaviour'' familiar from linear response theory. Beyond this limit, deviations from Lorentzian behaviour are expected.

It is interesting to examine the steady state obtained for extreme levels of saturation. In such a case, the leading terms in the numerator and denominator are those corresponding to the highest order in ϵ. The following asymptotic values are then obtained:

$$\hat{P}_x^{ss}\rightarrow-\frac{\gamma_x}{\Gamma_x}\approx-\frac{1}{2}\tanh\left(\frac{\beta(2\epsilon)}{2}\right),$$

$$\hat{P}_x^{ss},\hat{P}_y^{ss}\rightarrow 0. \tag{D2}$$

The last equality on the first line is obtained by letting $|\sin(\theta)|\approx 1$, $\cos(\theta)\approx 0$, $\omega\pm\nu\approx\pm|2\epsilon|$ and $\nu\approx|2\epsilon|$. It therefore seems that for extremely intense fields (such that ϵ far exceeds ω_0) the steady-state polarization lies along the rotating driving field and its magnitude is what one would expect in thermal equilibrium for a stationary field whose magnitude equals the rotating field amplitude.

Finally, note that the power is given by $2\epsilon\omega\hat{P}_y^{ss}$. Hence, although $\hat{P}_y^{ss}$ vanishes at extreme saturation, the power does not because of the extra 2ϵ on the numerator. It can be shown that:

$$\mathscr{P}\rightarrow\frac{\Gamma_x\gamma_z+\Gamma_{zx}\gamma_x}{\Gamma_x}\approx\frac{1}{2}\,\omega\delta^0(\omega). \tag{D3}$$

The last equality is obtained in a similar manner to that in the equation for $\hat{P}_x^{ss}$ in Eq. (D2). The line-shape then turns out to be proportional to $\tilde{C}_{\Lambda\Lambda^\dagger}(\omega)$ and scanning through the frequencies at extreme saturation may provide information on the full dynamics of the bath fluctuations.

APPENDIX E: GENERAL PROPERTIES OF THE GENERALIZED POWER FUNCTION

In this Appendix it is shown that (a) the generalized power function vanishes when $\mathbf{\Lambda}$ and $\mathbf{\Lambda}^\dagger$ do; (b) the generalized power function is non-negative for all frequencies.

Consider the numerator on the rhs of Eq. (6.4). Substituting for α, Γ_p, η and δ their explicit definitions from Eq. (4.30), one obtains

$$
\begin{aligned}
&-2\epsilon\omega\nu(\alpha\Gamma_p+\eta\delta)\\
&\quad=2\omega\epsilon^2\{\tfrac{1}{4}\sin^2(\theta)[\tilde{C}_{\Lambda\Lambda^\dagger}(\omega+\nu)\tilde{C}_{\Lambda\Lambda^\dagger}(\omega-\nu)(1-e^{-2\beta\omega})+\tfrac{1}{2}\tilde{C}_{\Lambda\Lambda^\dagger}(\omega)\tilde{C}_{\Delta\Delta}(\nu)(1+e^{-\beta\nu})(1-e^{-\beta\omega})]+\tfrac{1}{2}[1-\cos(\theta)]^2\\
&\qquad\times[\tfrac{1}{4}\tilde{C}_{\Lambda\Lambda^\dagger}(\omega-\nu)\tilde{C}_{\Delta\Delta}(\nu)(1-e^{-\beta\omega})+\tfrac{1}{2}\tilde{C}_{\Lambda\Lambda^\dagger}(\omega)\tilde{C}_{\Lambda\Lambda^\dagger}(\omega-\nu)(1+e^{-\beta(\omega-\nu)})(1-e^{-\beta\omega})]+\tfrac{1}{2}[1+\cos(\theta)]^2\\
&\qquad\times[\tfrac{1}{4}\tilde{C}_{\Lambda\Lambda^\dagger}(\omega+\nu)\tilde{C}_{\Delta\Delta}(\nu)e^{-\beta\nu}(1-e^{-\beta\omega})+\tfrac{1}{4}\tilde{C}_{\Lambda\Lambda^\dagger}(\omega)\tilde{C}_{\Lambda\Lambda^\dagger}(\omega+\nu)(1+e^{-\beta(\omega+\nu)})(1-e^{-\beta\omega})]\}. \qquad \text{(E1)}
\end{aligned}
$$

As $\mathbf{\Lambda}$ and $\mathbf{\Lambda}^\dagger$ vanish, so do $\tilde{C}_{\Lambda\Lambda^\dagger}(\omega)$ and $\tilde{C}_{\Lambda\Lambda^\dagger}(\omega\pm\nu)$, so that the power also vanishes. Since $C_{\Lambda\Lambda^\dagger}$ and $C_{\Delta\Delta}$ are non-negative the numerator, Eq. (E1), is also positive for all field frequencies, including negative ones!

A similar general proof for the non-negativity of the denominator on the rhs of Eq. (6.4) is impossible. To see this, note that all the bath parameters appearing in the denominator are either functions of ω and 0 or of $\omega\pm\nu$ and ν (cf. Tables I and II). The denominator may be broken into separate products, each consisting of three bath parameters. These products may be grouped according to their consistency of ω and 0 dependent bath parameters and $\omega\pm\nu$ and ν dependent bath parameters. The sum of members of each group should separately be non-negative if the denominator is to be non-negative, since the group's members are independent of one another.

Consider the group of terms containing three $\omega\pm\nu$ and ν dependent bath parameters. The sum of these terms is $\Gamma_p(\frac{1}{4}\Gamma_p^2-\lambda^2)$. Since $\Gamma_p\geqslant 0$, the non-negativity of this term is equivalent to the non-negativity of $(\frac{1}{4}\Gamma_p^2-\lambda^2)$. The latter is given by

$$
\begin{aligned}
\tfrac{1}{4}\Gamma_p^2-\lambda^2=&\tfrac{1}{4}\cos(\theta)[\cos^4(\theta/2)\Gamma_p^{02}(\omega+\nu)-\sin^4(\theta/2)\\
&\times\Gamma_p^{02}(\omega-\nu)]+\tfrac{1}{2}\sin^2(\theta)\Gamma_d'^{0}[\cos^2(\theta/2)\\
&\times\Gamma_p^{0}(\omega+\nu)+\sin^2(\theta/2)\Gamma_p^{0}(\omega-\nu)]. \qquad \text{(E2)}
\end{aligned}
$$

Thus, the contribution of this independent group is not necessarily non-negative. The same conclusion is arrived at when considering the other groups.

The way out of this seeming inconsistency is by an analysis of the denominator in light of the approximation that $\gamma_1\ldots\gamma_9<<\omega$, which was introduced in the derivation of the master equation. To see this note that the first term in the denominator, $\Gamma_p\nu^2$, is positive since $\Gamma_p>0$. Note that this term is the only one in the denominator that is first order in the bath parameters (Γ_p) and second order in the field parameters ($\Delta\omega$ and ϵ). The other terms are of third order in the bath parameters. A few cases are now considered.

(1) $|\Delta\omega|\sim\omega$. In such a case, $|\Delta\omega|>>\Gamma_p,\Gamma_d',\eta,\xi$ and λ, and hence the sign of the denominator is determined by the sign of the first positive term.

(2) $\Delta\omega=0$. There are two possibilities in this case.

(a) $|2\epsilon|\sim\omega_0$. In such a case, $|2\epsilon|>>\Gamma_p,\Gamma_d',\eta,\xi,\lambda$. Hence, the sign of the denominator is determined by that of the term proportional in $(2\epsilon)^2$.

(b) $|2\epsilon|<<|\omega_0|$. In such a case 2ϵ may be of the same order of magnitude or smaller than $\Gamma_p,\Gamma_d',\eta,\xi$ and λ. However, the limit $\Delta\omega=0,|2\epsilon|<<\omega_0$ was already considered in Sec. V and the corresponding line-shape converges to that predicted by the SBE.

In conclusion the power is always positive within the approximations of the model. Hence, the model is consistent with the second law of thermodynamics.

[1] F. Bloch, Phys. Rev. **70**, 460 (1946).
[2] R. K. Wangsness and F. Bloch, Phys. Rev. **89**, 728 (1953).
[3] A. G. Redfield, IBM J. **19**, 1 (1957).
[4] A. Abragam, *The Principles of Nuclear Magnetism* (Oxford University, Oxford, 1961).
[5] C. P. Slichter, *Principles of Magnetic Resonance* (Springer, Berlin, 1990).
[6] R. R. Ernst, G. Bodenhausen, and A. Wokaun, *Principles of Nuclear Magnetic Resonance in One and Two Dimensions* (Oxford University, Oxford, 1990).
[7] R. Kubo and K. Tomita, J. Phys. Soc. Jpn. **9**, 889 (1954).
[8] L. Allen and J. Eberly, *Optical Resonance and Two-Level Atoms* (Dover, New York, 1987).
[9] W. H. Louisell, *Quantum Statistical Properties of Radiation* (Wiley, New York, 1990).
[10] C. Cohen-Tannoudji, B. Diu, and F. Laloe, *Quantum Mechanics* (Wiley, New York, 1977).
[11] D. J. Diestler, Mol. Phys. **32**, 1091 (1976).
[12] D. W. Oxtoby, Annu. Rev. Phys. Chem. **32**, 77 (1981).
[13] J. L. Skinner and D. Hsu, Adv. Chem. Phys. **65**, 1 (1986).
[14] R. Silbey, in *Relaxation Processes in Molecular Excited States*, edited by J. Funfchilling (Clauser Academic, New York, 1989).
[15] V. Romero-Rochin and I. Oppenheim, Physica A **155**, 52 (1989).
[16] B. B. Laird, J. Budimir, and J. L. Skinner, J. Chem. Phys. **94**, 4391 (1991).
[17] T. M. Chang and J. L. Skinner, Physica A **193**, 483 (1993).
[18] A. G. Redfield, Phys. Rev. **98**, 1787 (1955).
[19] F. Bloch, Phys. Rev. **105**, 1206 (1957).
[20] K. Tomita, Prog. Theor. Phys. **19**, 541 (1958).
[21] P. S. Hubbard, Rev. Mod. Phys. **33**, 249 (1961).
[22] P. N. Argyres and P. L. Kelley, Phys. Rev. **134**, A98 (1964).
[23] R. G. DeVoe and R. G. Brewer, Phys. Rev. Lett. **50**, 1269 (1983).
[24] A. G. Yodh, J. Golub, N. W. Carlson, and T. W. Mossberg, Phys. Rev. Lett. **53**, 659 (1984).
[25] E Hanamura, J. Phys. Soc. Jpn. **52**, 2258 (1983).
[26] E Hanamura, J. Phys. Soc. Jpn. **52**, 3265 (1983).
[27] E Hanamura, J. Phys. Soc. Jpn. **52**, 3678 (1983).
[28] M. Yamanoi, in *Coherence and Quantum Optics V*, edited by L. Mandel and E. Wolf (Plenum, New York, 1984).
[29] M. Yamanoi and J. H. Eberly, J. Opt. Soc. Am. B **1**, 751 (1984).
[30] A. Schenzle, M. Mitsunaga, R. G. DeVoe, and R. G. Brewer, Phys Rev. A **30**, 325 (1984).
[31] K. Wodkiewicz and J. H. Eberly, Phys. Rev. A **32**, 992 (1985).
[32] P. R. Berman and R. G. Brewer, Phys. Rev. A **32**, 2784 (1985).
[33] S. Ya Kilin and A. P. Nizovtsev, J. Phys. B **19**, 3457 (1986).
[34] M. Yamanoi and J. H. Eberly, Phys. Rev. A **34**, 1609 (1986).
[35] R. Boscaino and V. M. La Bella, Phys. Rev. A **41**, 5171 (1990).
[36] R. Boscaino and F. M. Gelardi, Phys. Rev. A **45**, 546 (1992).
[37] S. Carnot, *Réflections sur la Puissance Motrice du Feu et sur les Machines propres à Développer cette Puissance* (Bachelier, Paris, 1824).
[38] H. B. Callen, *Thermodynamics* (Wiley, New York, 1979).
[39] L. Boltzmann, *Lectures on Gas Theory* (translated by S. G. Brush) (University of California, Berkeley, 1964).
[40] R. Kubo, M. Toda, and N. Hashitsume, *Statistical Physics II-Nonequilibrium Statistical Mechanics* (Springer, Berlin, 1983).

[41] R. Alicki and K. Lendi, *Quantum Dynamical Semigroups and Applications* (Springer, Berlin, 1987).
[42] R. Kosloff, J. Chem. Phys. **80**, 1625 (1984).
[43] E. Geva and R. Kosloff, J. Chem. Phys. **96**, 3054 (1992).
[44] E. Geva and R. Kosloff, J. Chem. Phys. **97**, 4398 (1992).
[45] E. Geva and R. Kosloff, Phys. Rev. E **49**, 3903 (1994).
[46] H. Spohn and J. L. Lebowitz, Adv. Chem. Phys. **38**, 109 (1979).
[47] R. Alicki, J. Phys. A **12**, L103 (1979).